

Karoo BioGaps report: Scorpion occupancy models

Dominic Henry

11 April 2018

Contents

1	Summary	2
2	Detection process	3
3	Occupancy process	5
4	Species richness	9
4.1	Species richness at sampled sites	9
4.2	Number of occupied sites by each species	10
4.3	Species richness and standard deviation map	11
5	Species occurrence maps	12
5.1	Maps of mean occurrence for individual species	12
5.2	Maps of standard deviation of mean occurrence for individual species	21
6	Appendices	30
6.1	Appendix A - Species list	30
6.2	Appendix B - Covariate maps	31
6.3	Appendix C - Model diagnostics	33

1 Summary

The scorpion team, led by Lorenzo Perдини, carried out three sampling field trips in February 2017, December 2017 and February 2018, respectively. In total the team managed to visit the 30 essential pentads. Using a double-observer protocol they completed 110 transects in which they recorded 25 species from three families (*Buthidae*, *Hormuridae* and *Scorpionidae*). See Appendix A for a full list of species recorded in the surveys. Excitingly, the team captured a specimen from the *Opisthophthalmus* genus which, as of yet, remains undescribed. The team used a combination of diurnal active searching (rock-flipping, burrow-excavating) and nocturnal search surveys.

Species were modelled as a random effect in the analysis which meant we were able to determine occupancy and detection probabilities for both individual species and the larger scorpion community as a whole. Mean community-level occupancy probability was fairly low ($\psi = 0.1$) while mean detection probability was moderate ($p = 0.5$). It was clear that there was substantial variation in these occupancy and detection probability estimates between species ($\psi_{SD} = 0.8$ and $p_{SD} = 0.74$).

The table below shows the estimates and the associated uncertainty (95% credible intervals) of occupancy and detection parameters.

Parameter	Mean	Lower 95% CI	Upper 95% CI
mu.psi	0.10	0.04	0.17
mu.p	0.50	0.35	0.63
sd.psi	0.80	0.69	0.89
sd.p	0.74	0.64	0.85

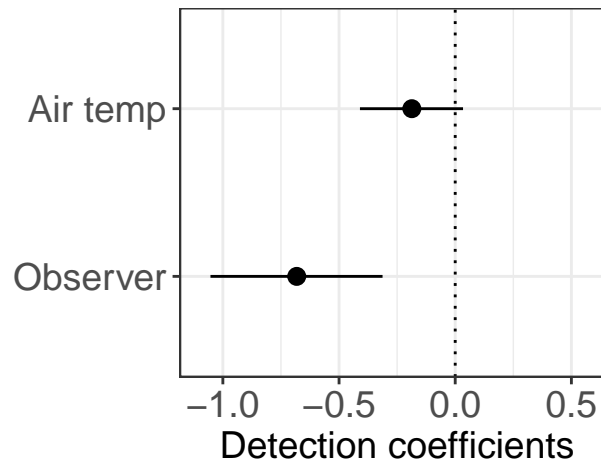
2 Detection process

Detection probability was modelled as a function of observer ID (LP or RC) and air temperature recorded during each survey. The equation for the detection sub-model can be written as

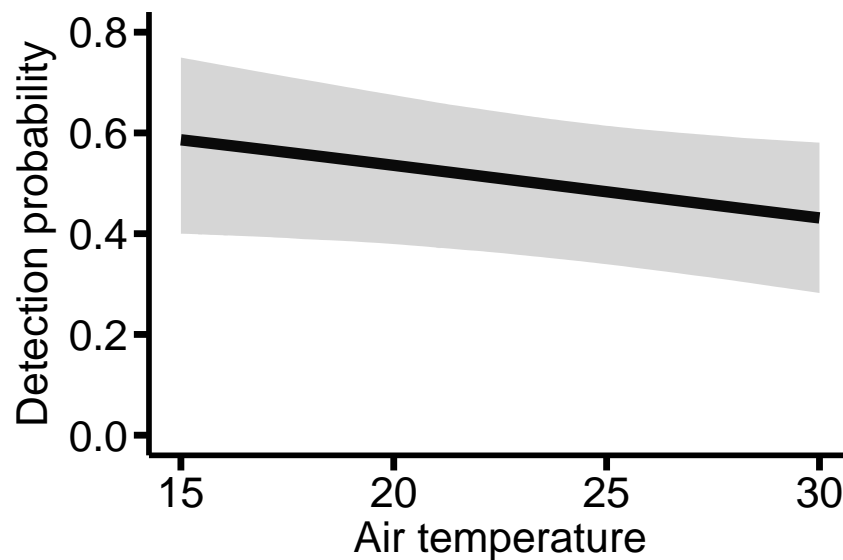
$$p_{ijk} = \alpha_0 + \alpha_1 * observerID_{ij} + \alpha_2 * airtemp_{ij}$$

where p_{ijk} is the detection probability of a species k at site i in survey j .

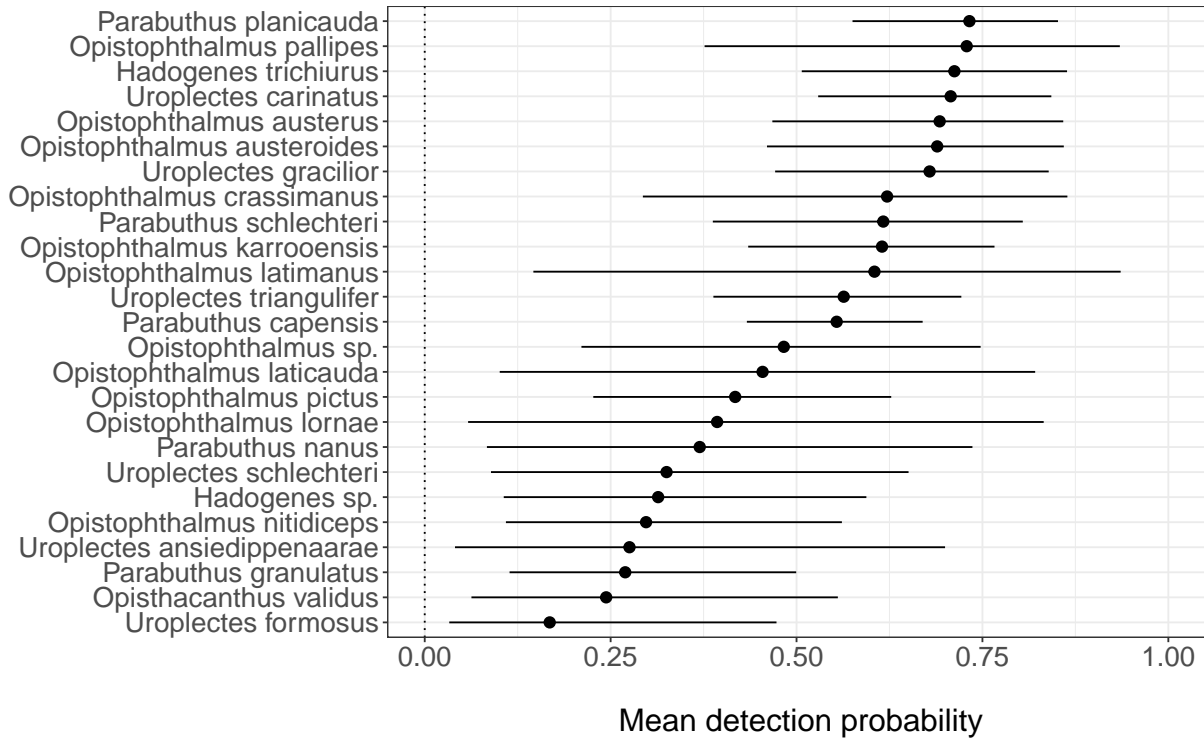
Below is a plot of the standardised magnitude of the detection coefficients (mean \pm 95% CI). The results show that detection probability increased as air temperature decreased. Species detectability differed with observer identification with observer 2 (RC) having a significantly lower coefficient.



The relationship between species detectability and air temperature can be visualised in the figure below showing the mean and 95% credible intervals.



Mean detection probability was calculated for each species and ranged from 0.17 to 0.73 with *Parabuthus planicauda* being the most detectable species and *Uroplectes formosus* being the least detectable. Below is a plot of mean detection for each species (plotted with the 95% credible intervals).



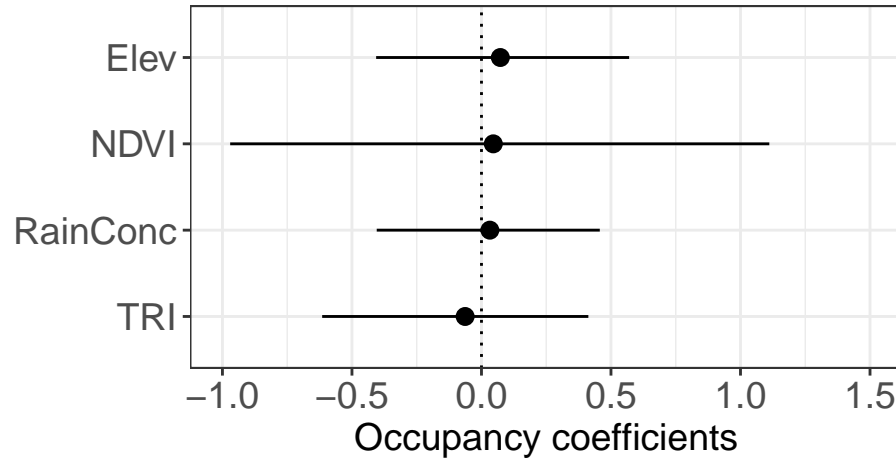
3 Occupancy process

Occupancy probability was modelled as a function of four covariates measured in each pentad: NDVI, rainfall concentration, elevation and terrain ruggedness index (TRI). See Appendix B for maps of each covariate illustrated across the BioGaps study area. The equation for the occupancy sub-model can be written as

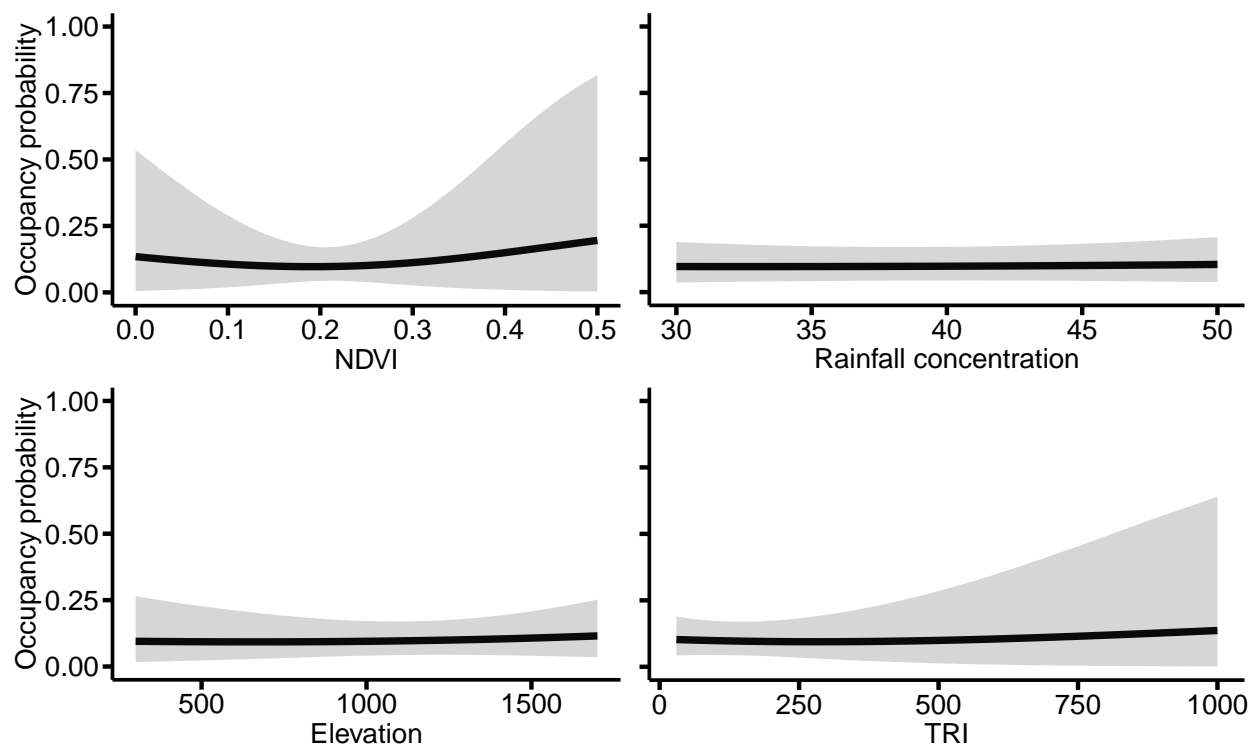
$$\psi_{ik} = \beta_0 + \beta_1 * NDVI_i + \beta_2 * rainConc_i + \beta_3 * elev_i + \beta_4 * TRI_i$$

where ψ_{ik} is the occupancy probability of a species k at site i .

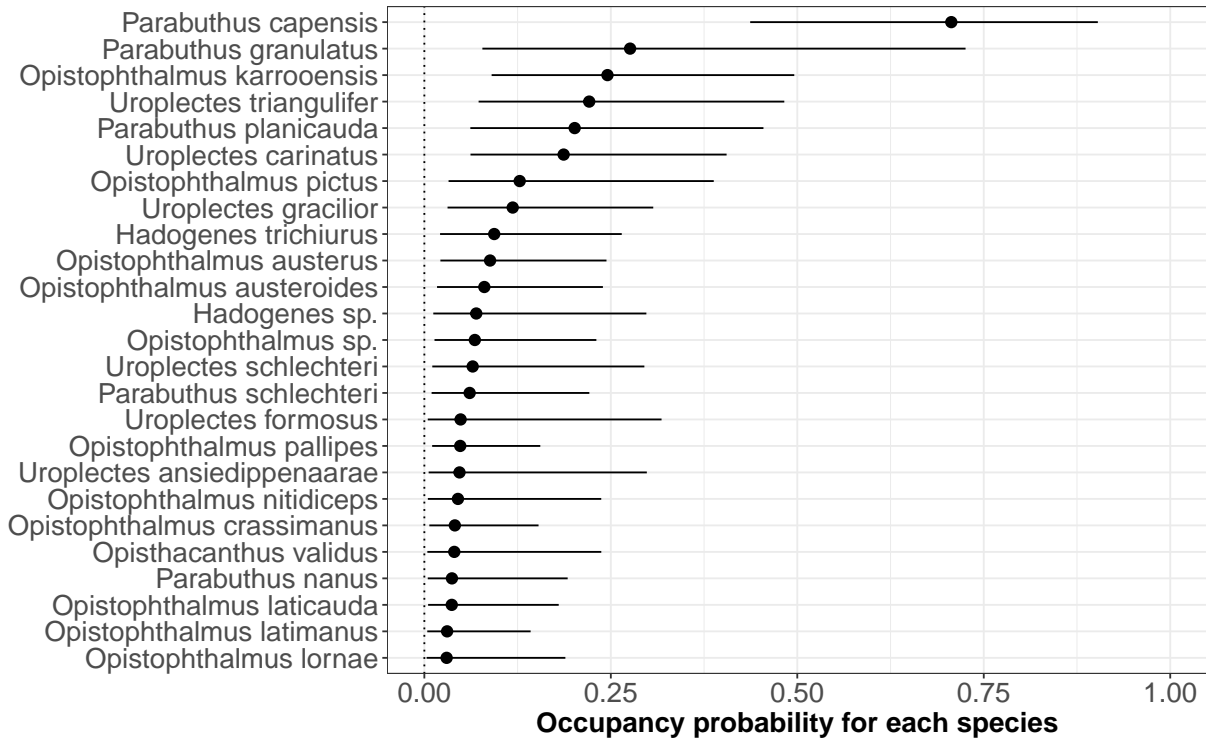
Below is a plot of the standardised magnitude of the each of the detection coefficients (mean \pm 95% CI). The results show that, at the community level, the environmental covariates are not significant predictors of species occupancy because the coefficients have CIs that overlap with zero. This does not mean that individual species themselves did not respond to environmental variables (see section on random effects below).



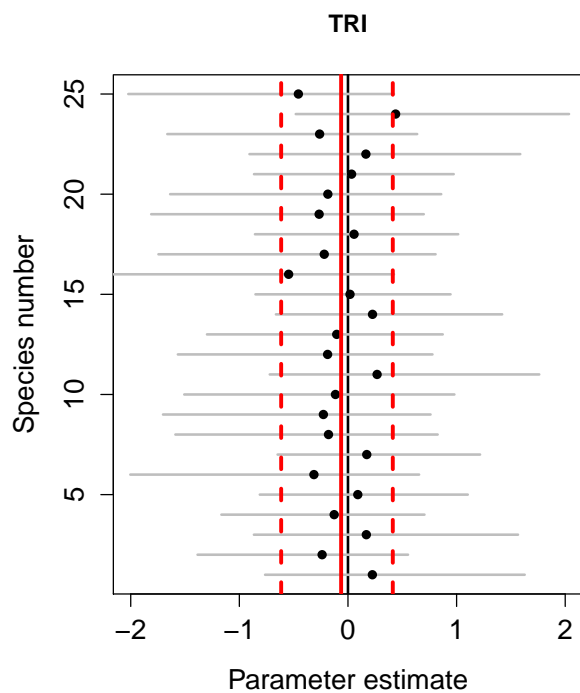
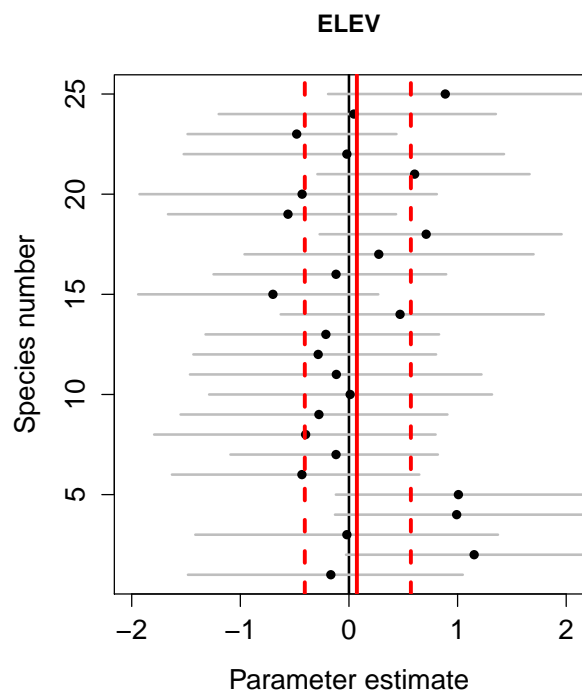
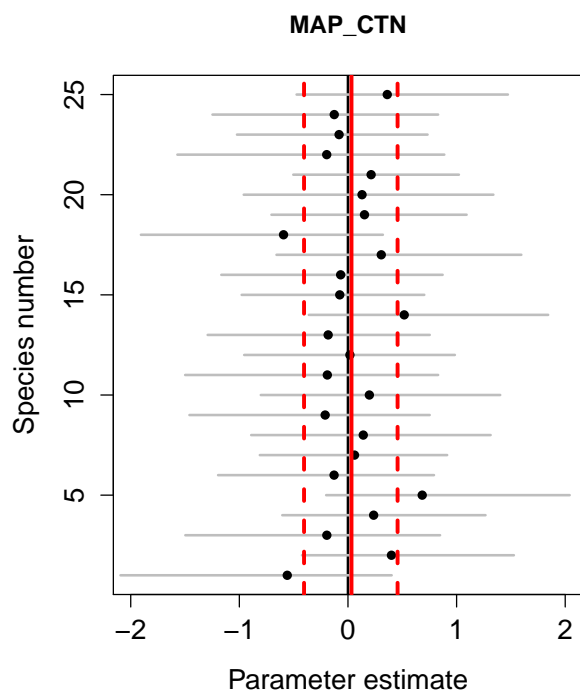
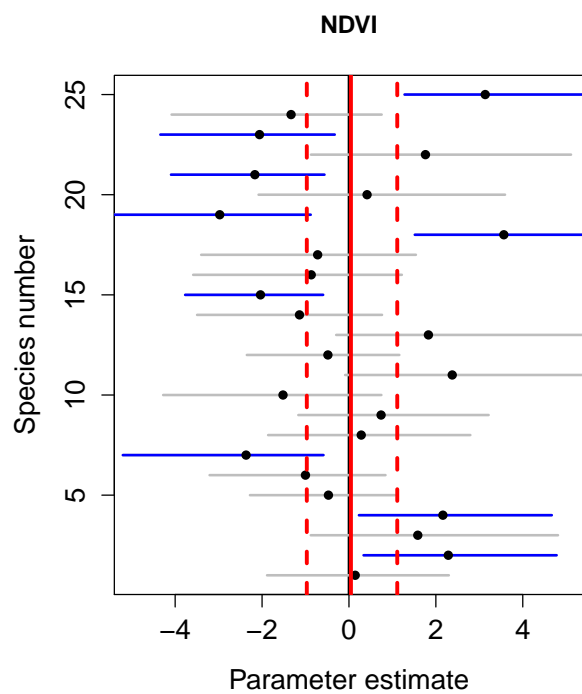
The relationship between species occupancy and NDVI, rainfall concentration, elevation and TRI can be visualised in the figure below showing the mean and 95% credible intervals.



Mean occupancy probability was calculated for each species and ranged from 0.03 to 0.71 with *Parabuthus capensis* having the highest occupancy and *Opisthophthalmus lornae* having the lowest. Below is a plot of mean detection for each species (plotted with the 95% credible intervals).



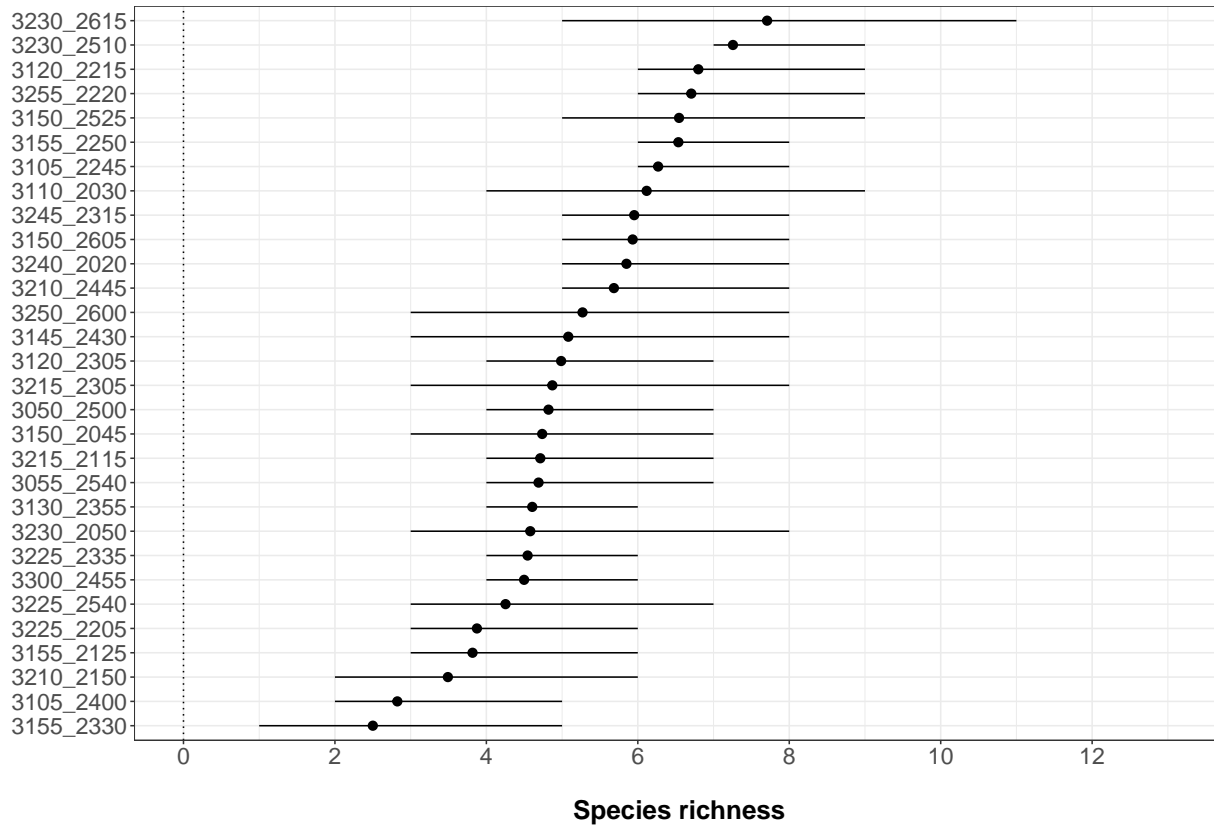
Species were modelled as a random effect in the occupancy models and so we were able to determine the relationship between occupancy and environmental covariates for each species. The plots below illustrate the species-level coefficients for the four environmental covariates. Blue lines indicate a significant relationship (i.e., 95% CIs do not overlap with zero). From the NDVI plot we can see that there were 4 species that had higher occupancy probability in areas with a higher primary productivity (with high NDVI) and 5 species that had a higher occupancy probability in dry areas with low primary productivity (low NDVI). There was little support for a significant relationship between occupancy and the remaining three covariates.



4 Species richness

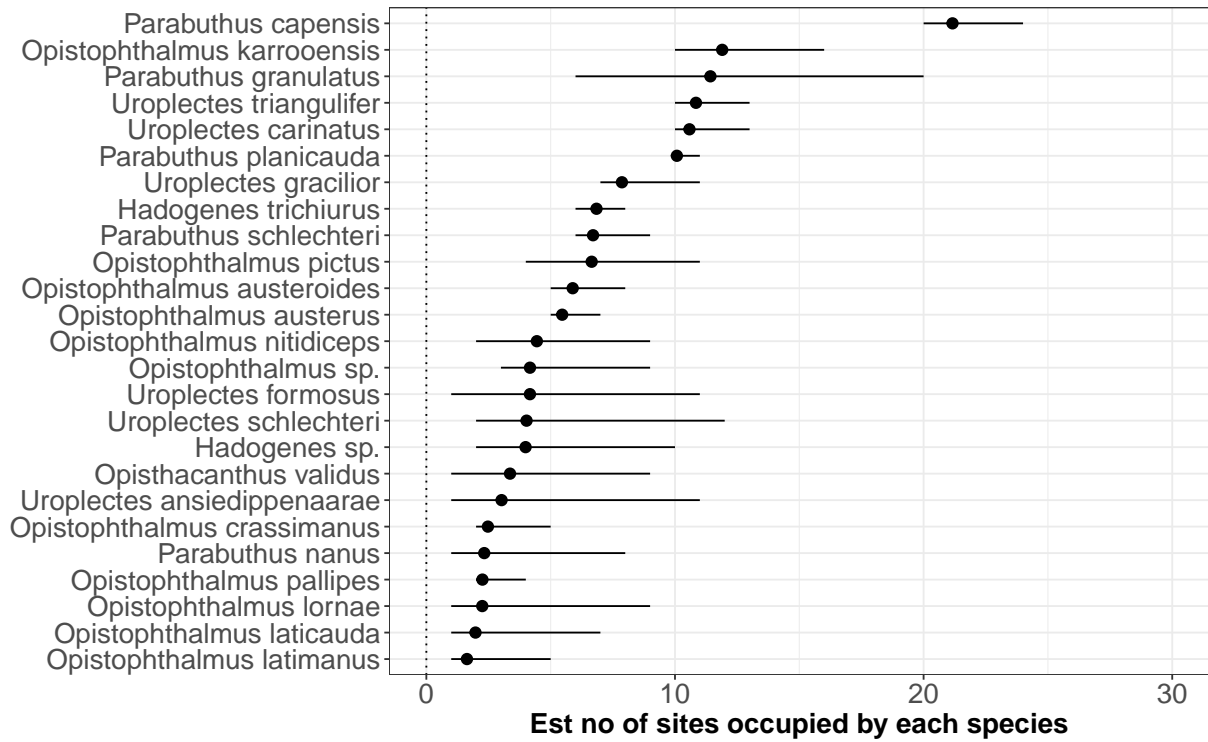
4.1 Species richness at sampled sites

Below is a plot of mean estimated species richness for each of the sampled pentads. They include the 95% CIs. The results show that richness was highest with 8 species in pentad 3230_2615 and lowest with 3 species in pentad 3155_2330.



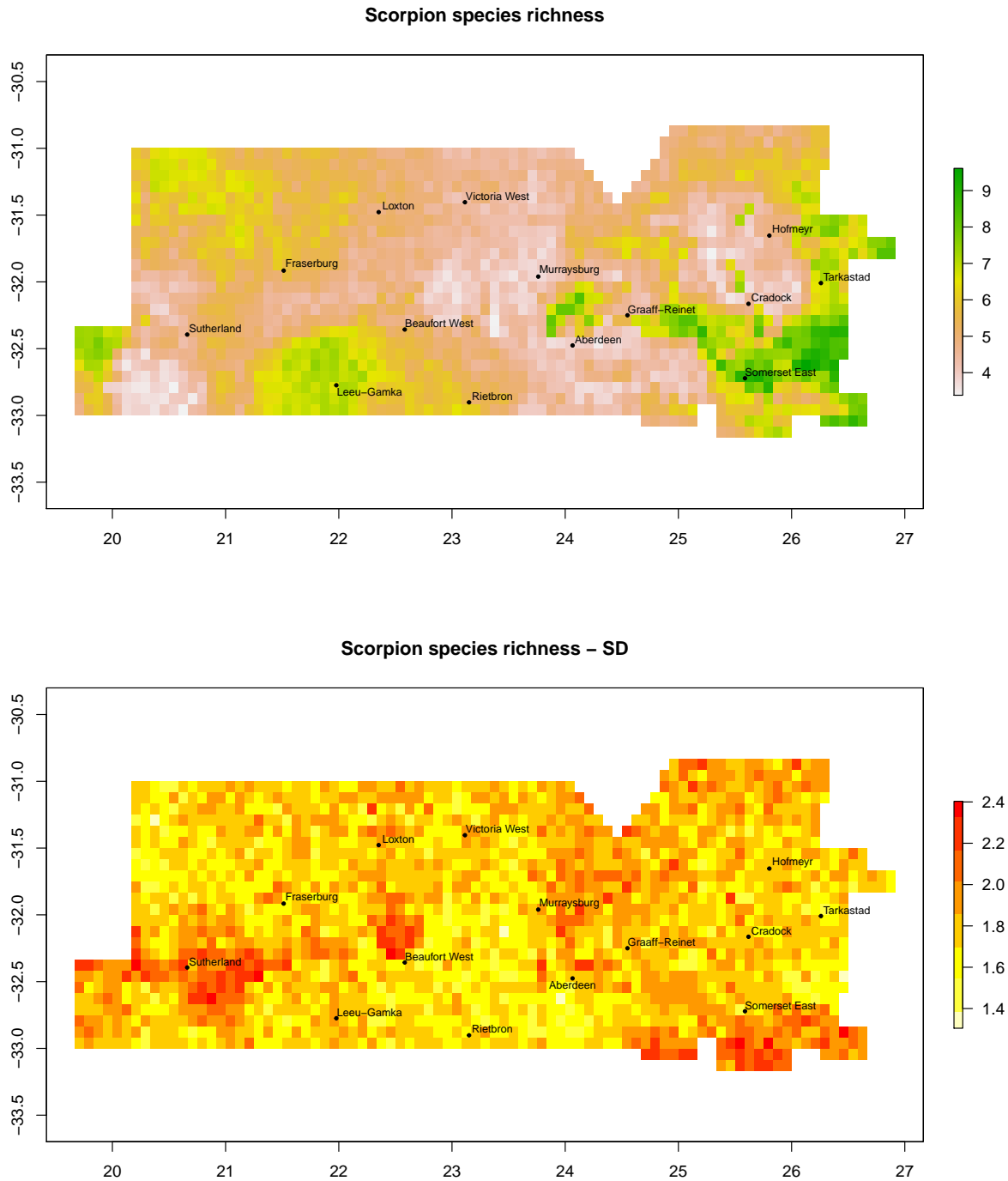
4.2 Number of occupied sites by each species

The models also allowed us to estimate the number of sites that the each species occurred within.



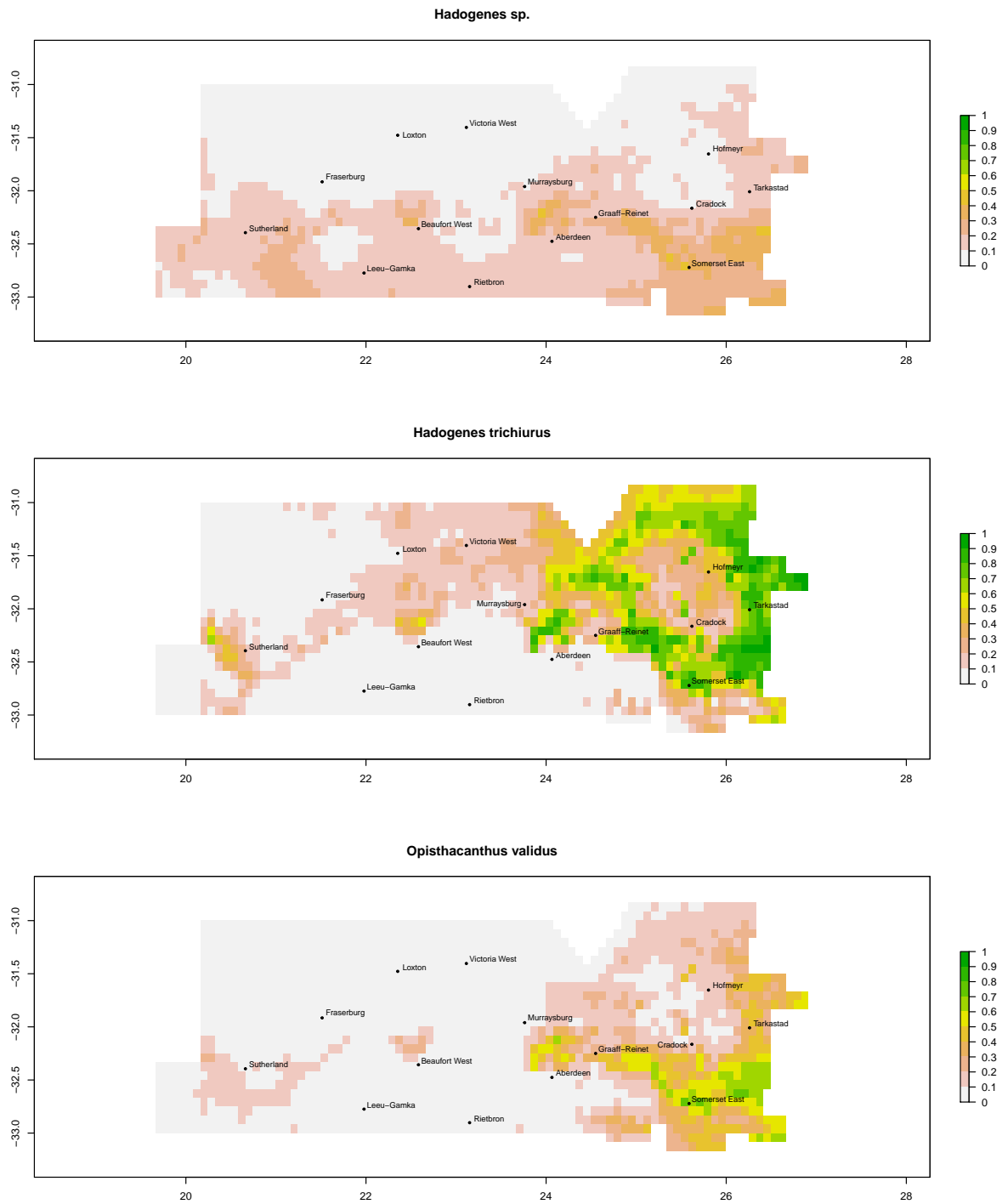
4.3 Species richness and standard deviation map

By combining the occupancy probability estimates of each species we were able to produce a predictive map of Scorpion species richness. The map below also shows the uncertainty associated with these estimates using standard deviation. Species richness was highest in the pentads located in the furthest eastern sections of the study area.

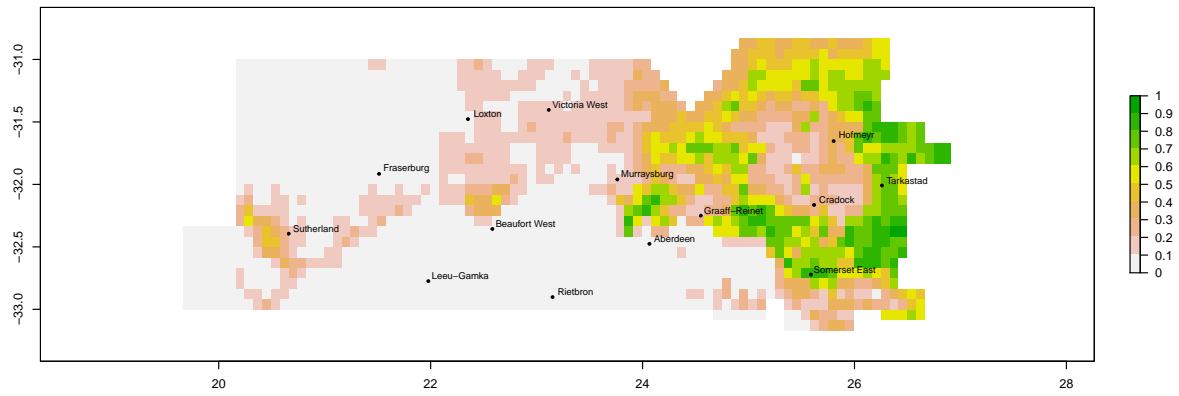


5 Species occurrence maps

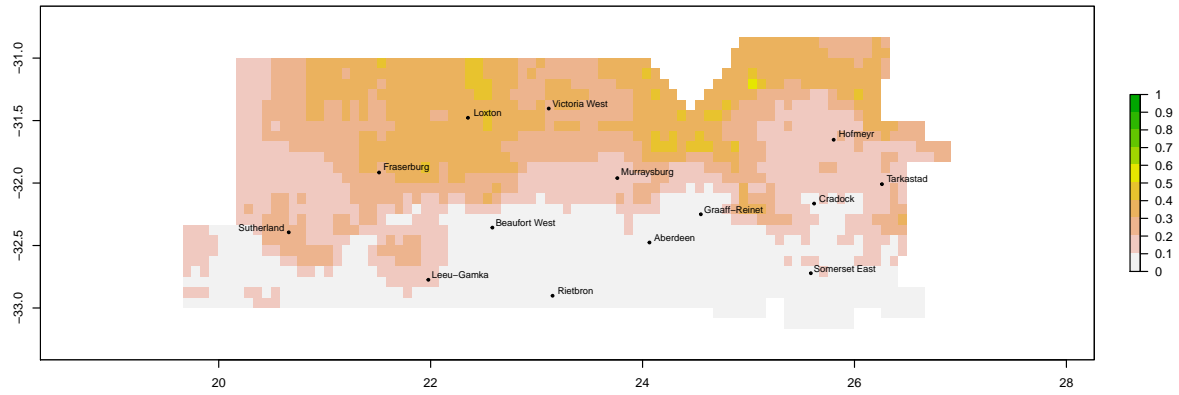
5.1 Maps of mean occurrence for individual species



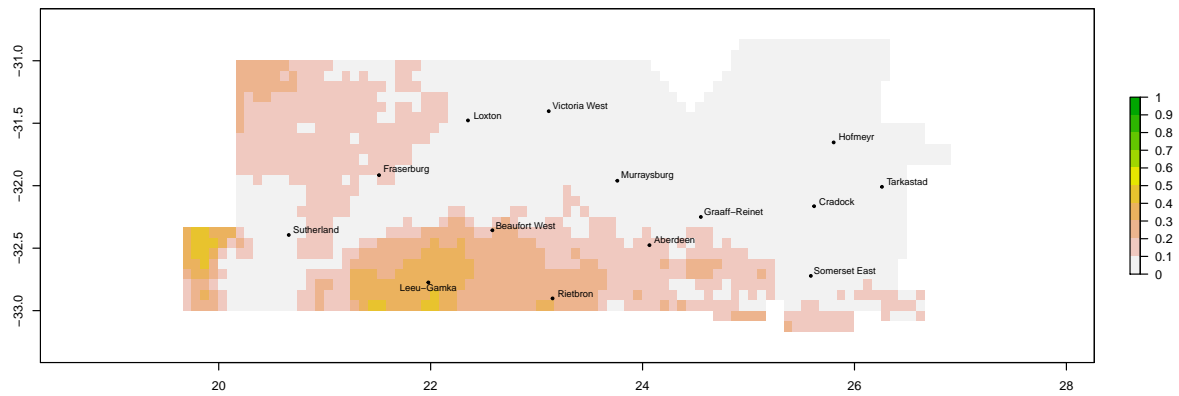
Opisthophthalmus austeroides



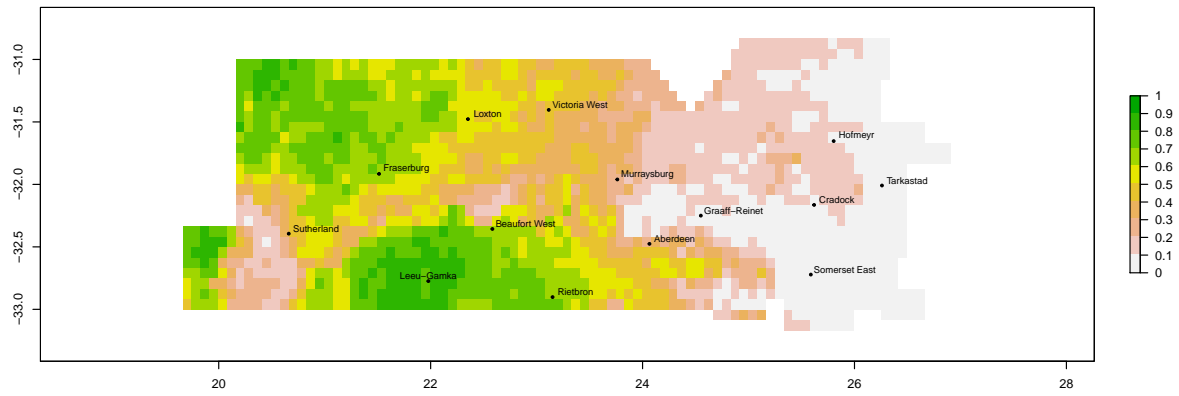
Opisthophthalmus austerus



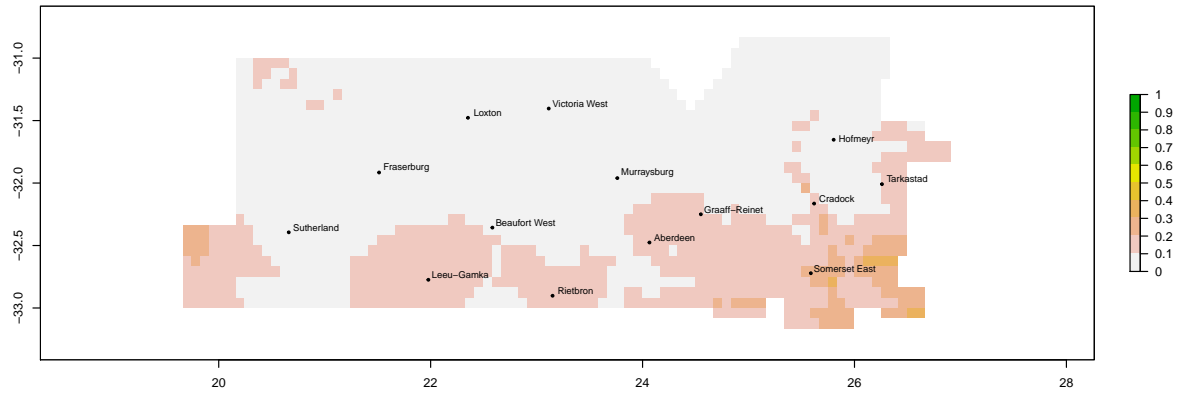
Opisthophthalmus crassimanus



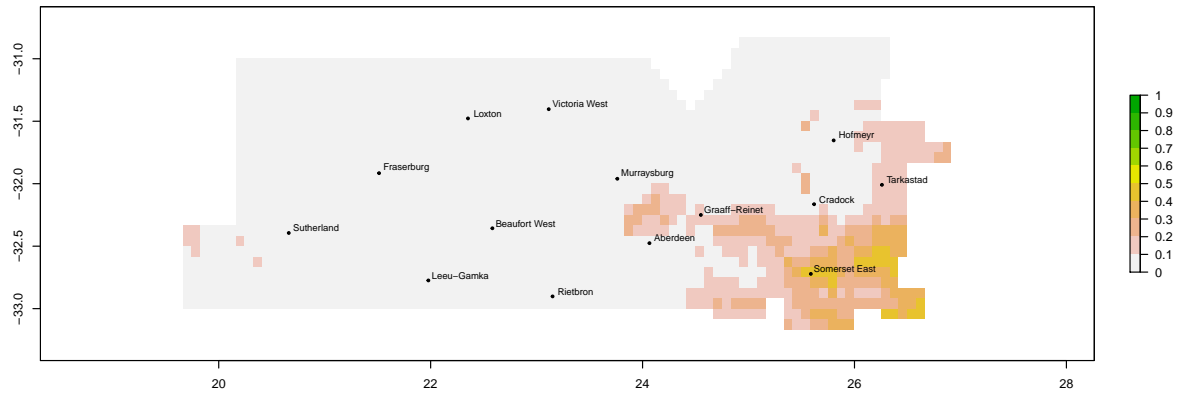
Opisthophthalmus karrooensis



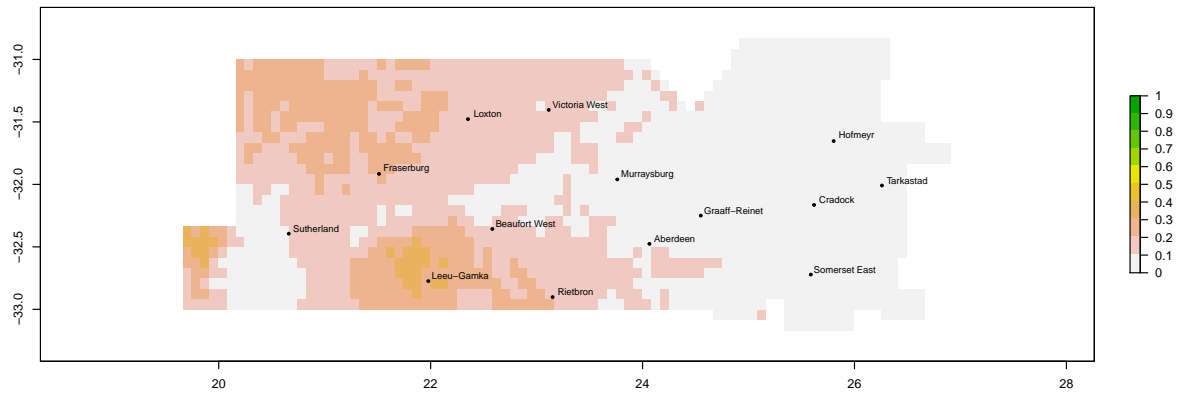
Opisthophthalmus laticauda



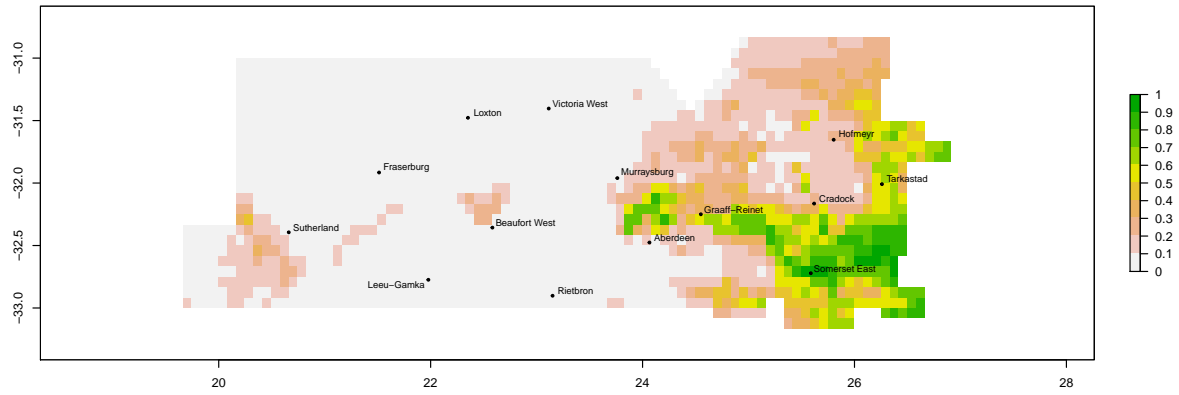
Opisthophthalmus latimanus



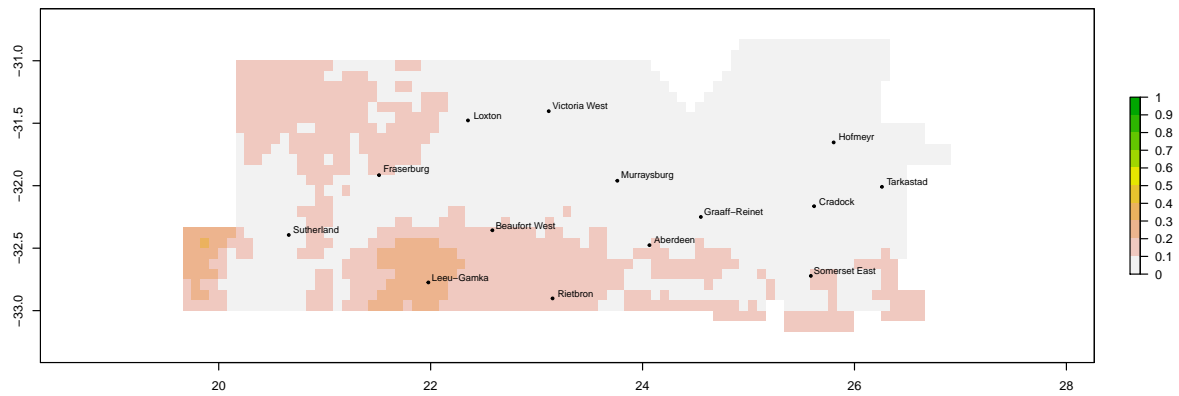
Opisthophthalmus lornae



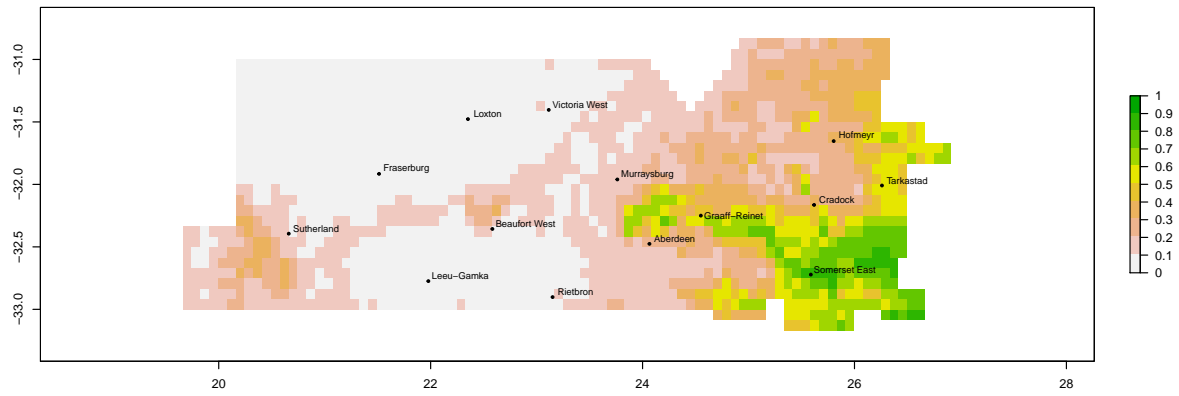
Opisthophthalmus nitidiceps



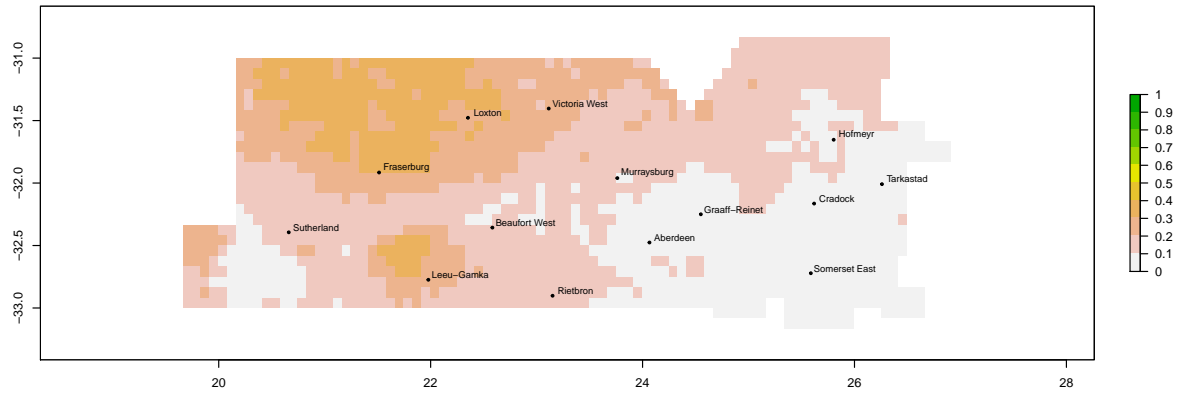
Opisthophthalmus pallipes



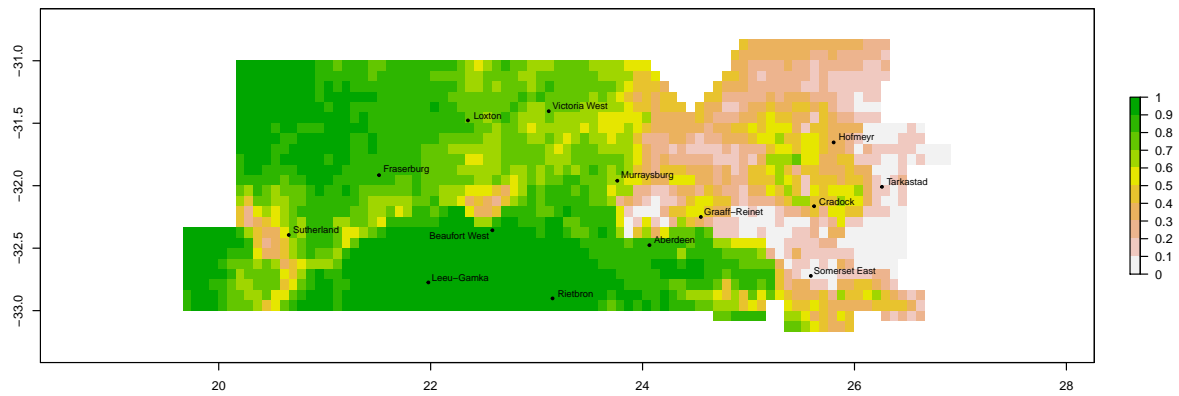
Opisthophthalmus pictus



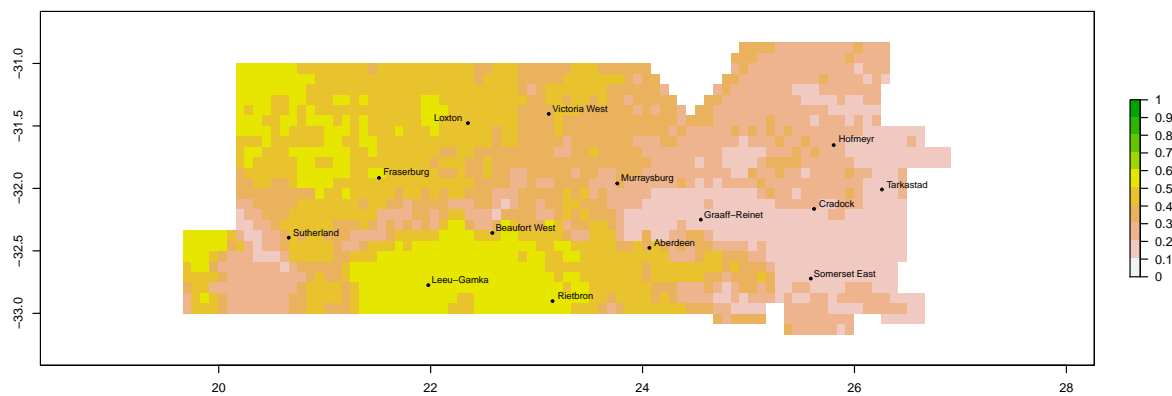
***Opisthophthalmus* sp.**



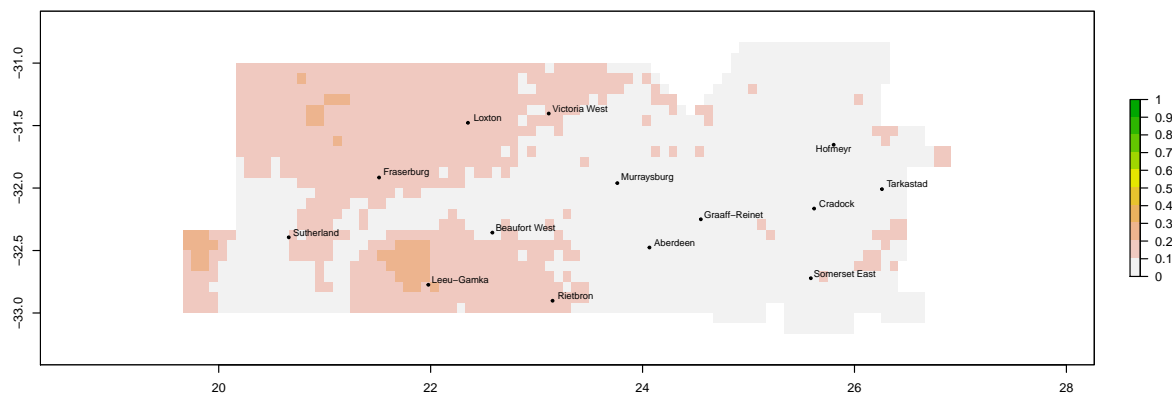
Parabuthus capensis



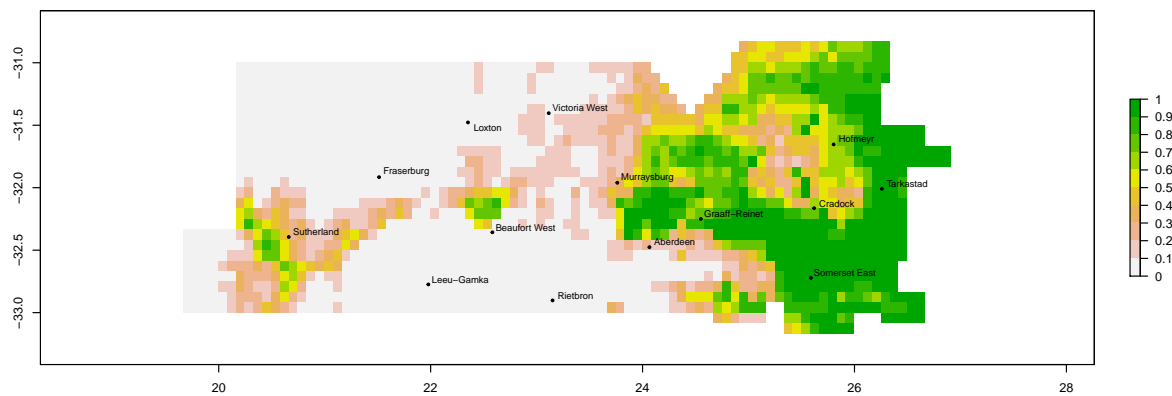
Parabuthus granulatus



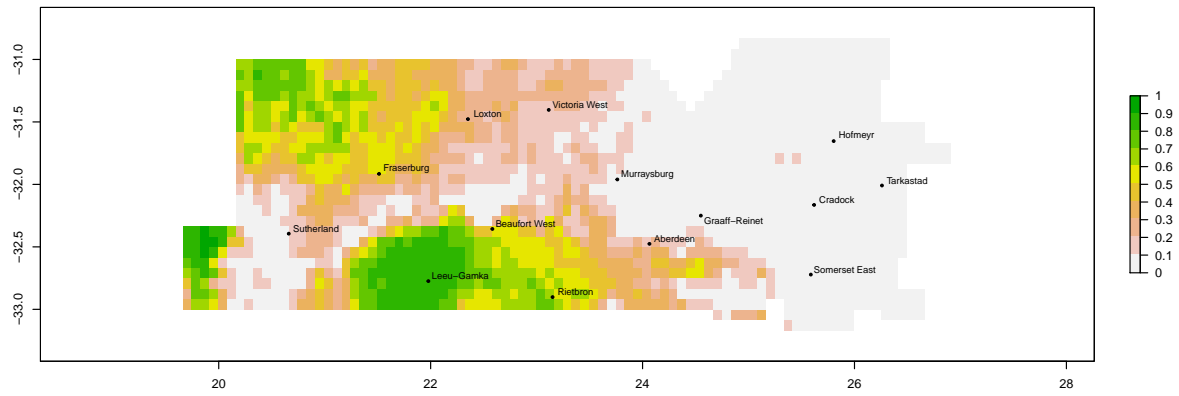
Parabuthus nanus



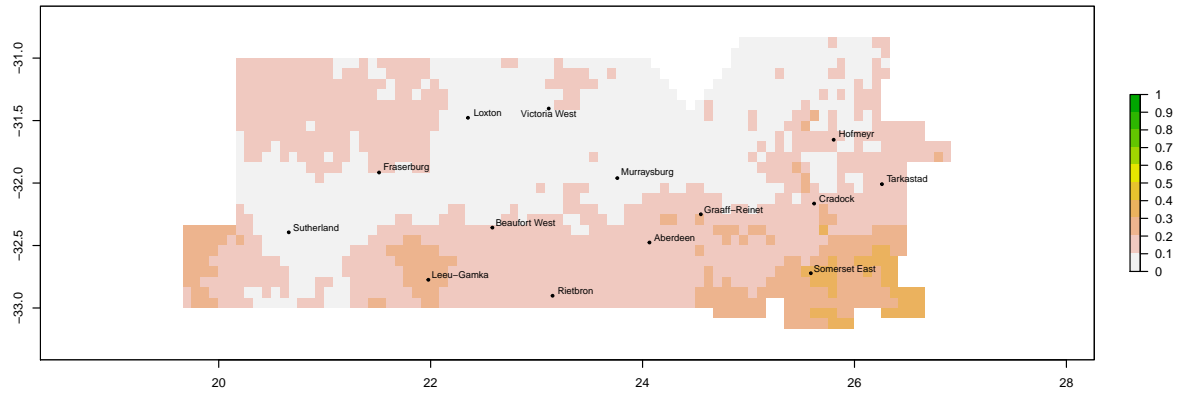
Parabuthus planicauda



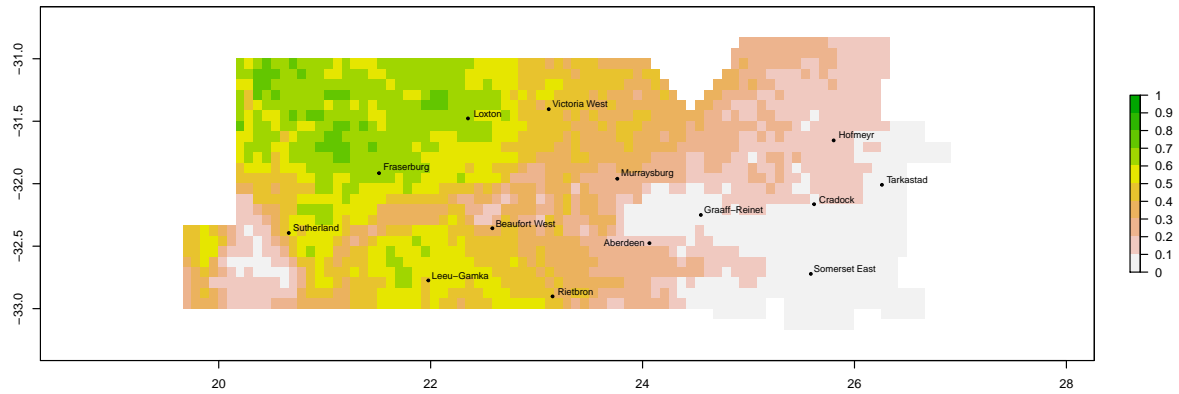
Parabuthus schlechteri



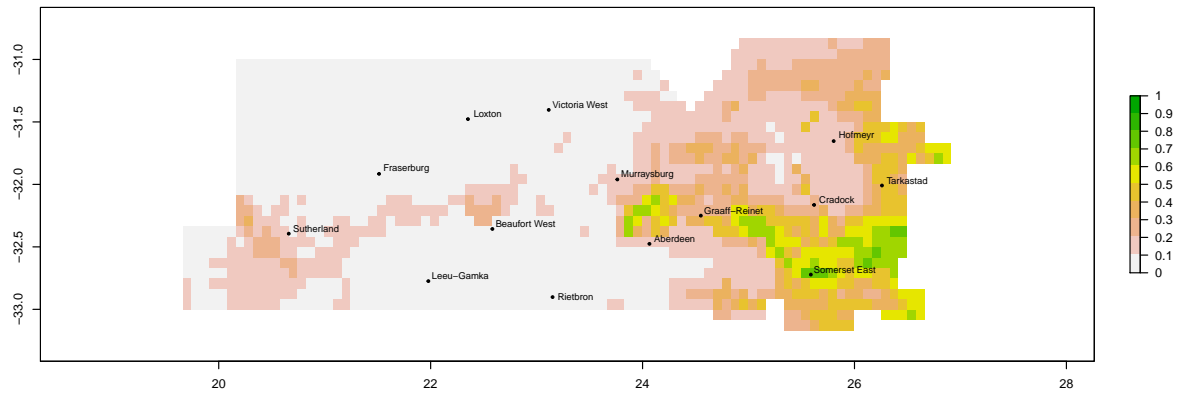
Uroplectes ansiedippenarae



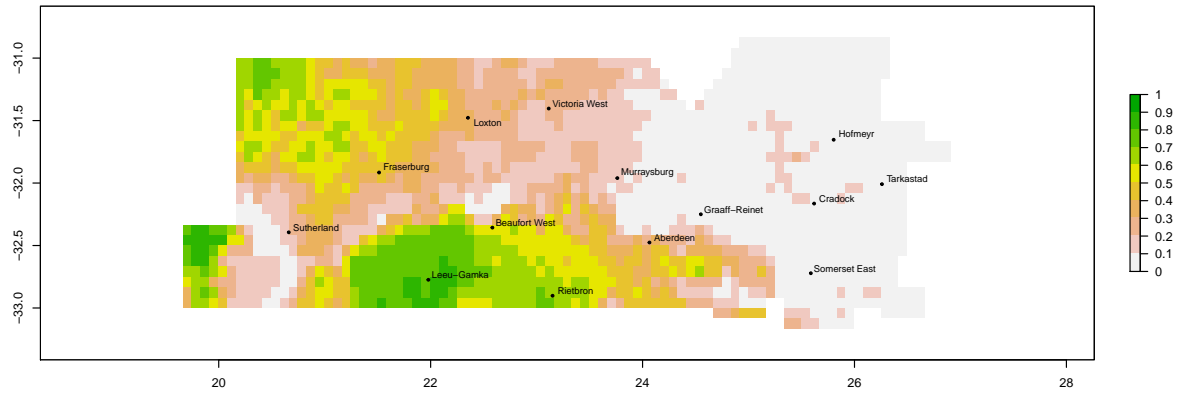
Uroplectes carinatus



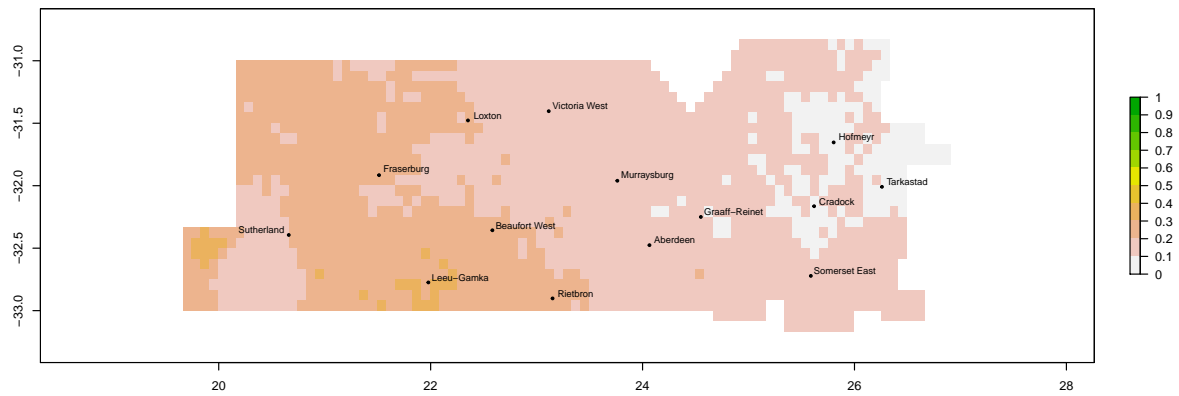
Uroplectes formosus



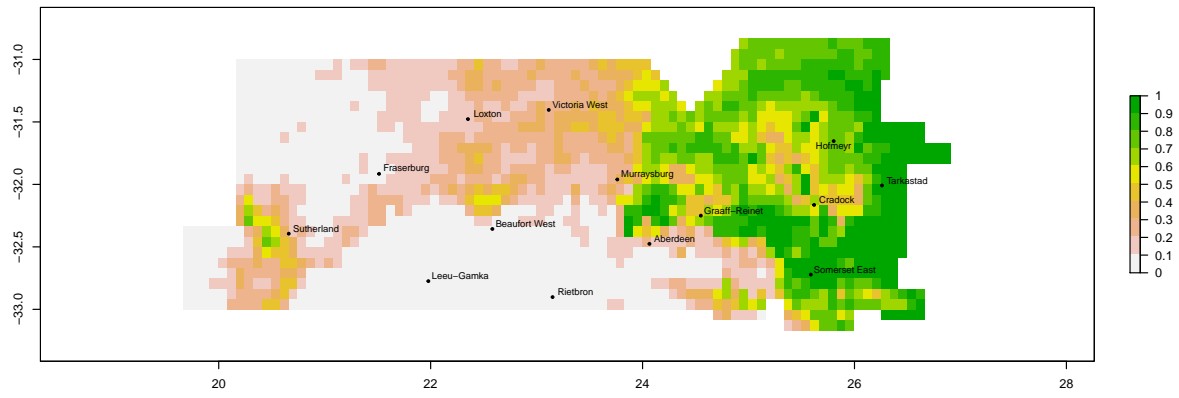
Uroplectes gracilior



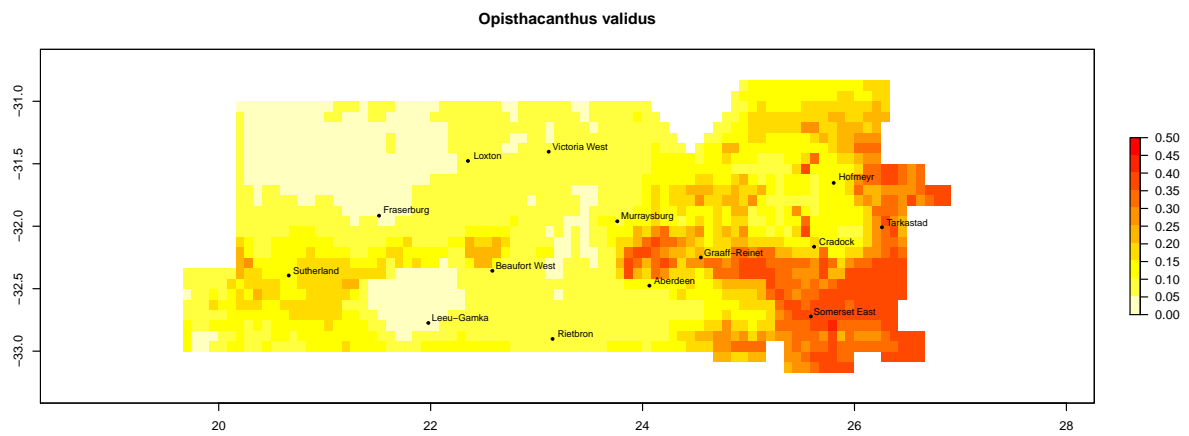
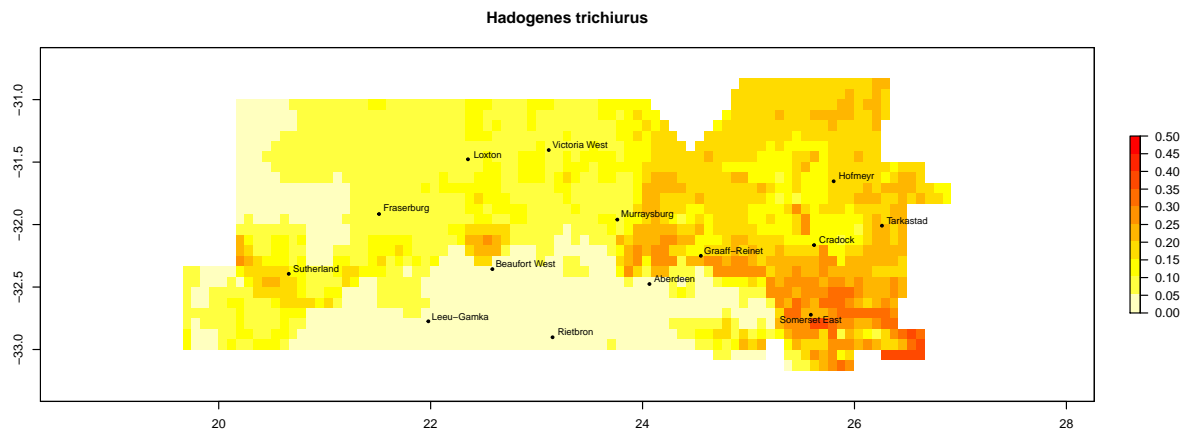
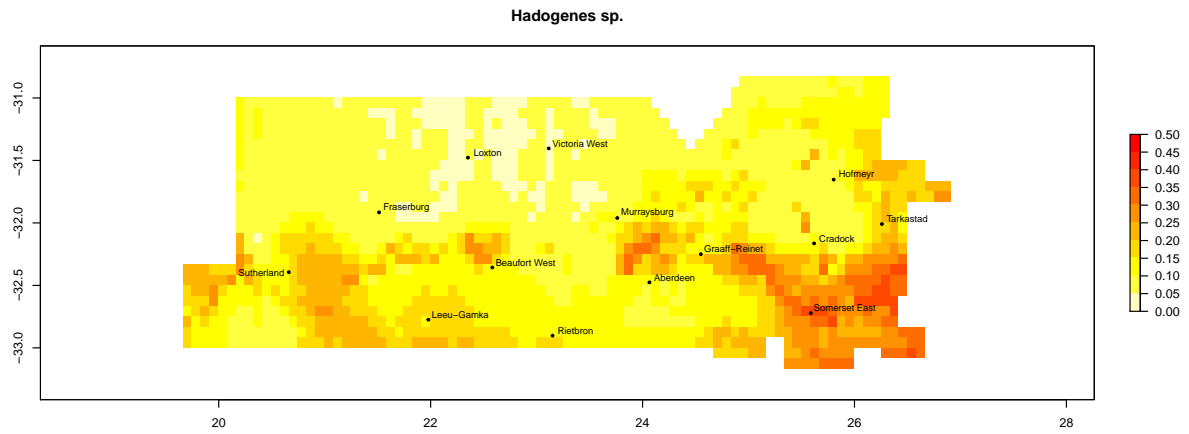
Uroplectes schlechteri



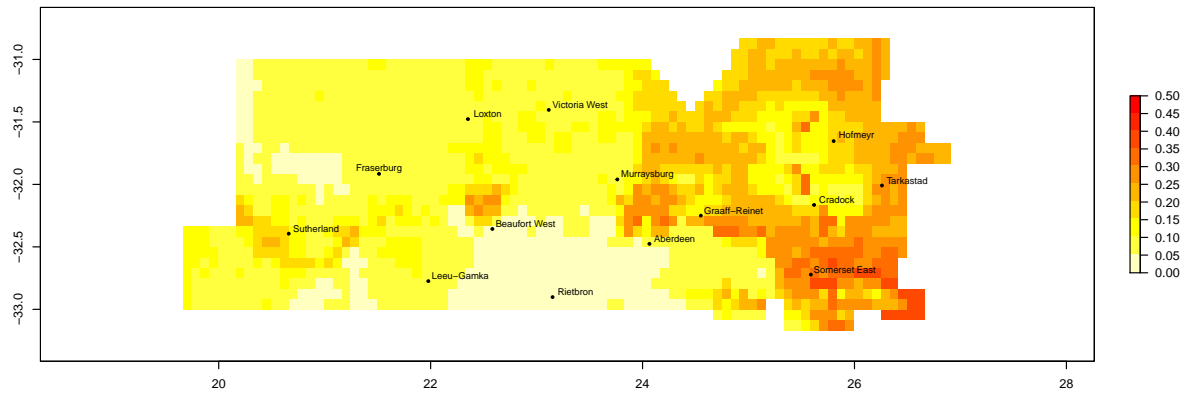
Uroplectes triangulifer



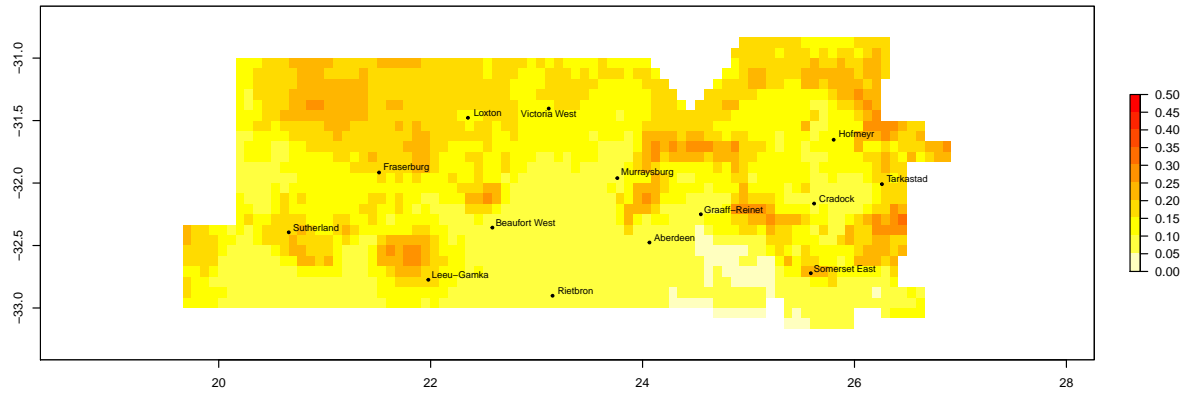
5.2 Maps of standard deviation of mean occurrence for individual species



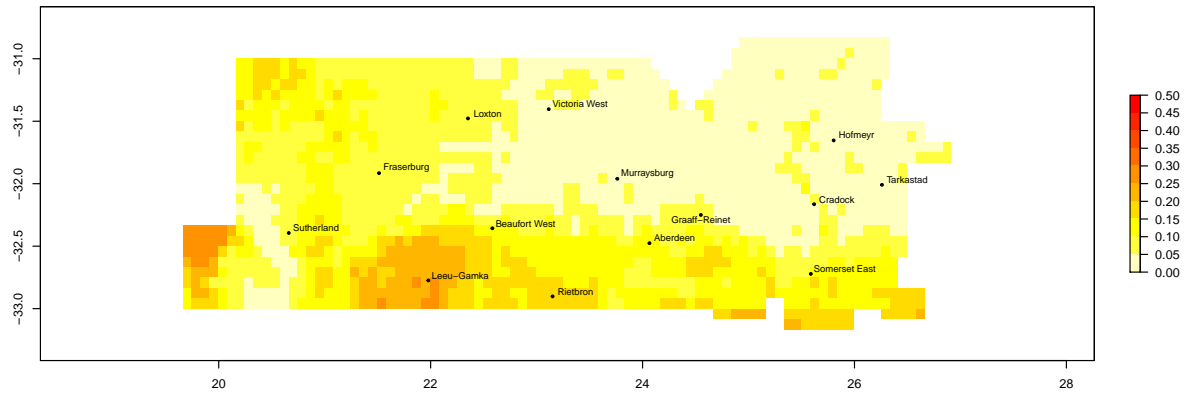
Opisthophthalmus austeroides



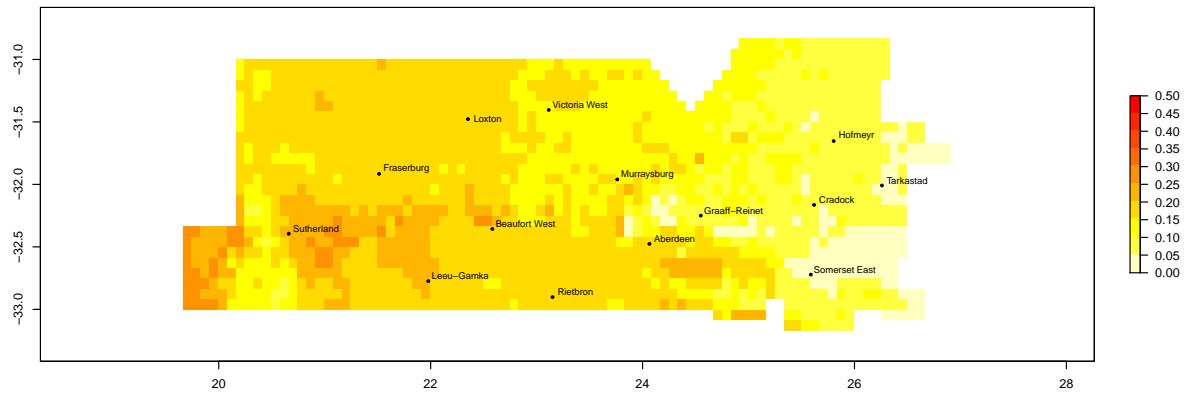
Opisthophthalmus austerus



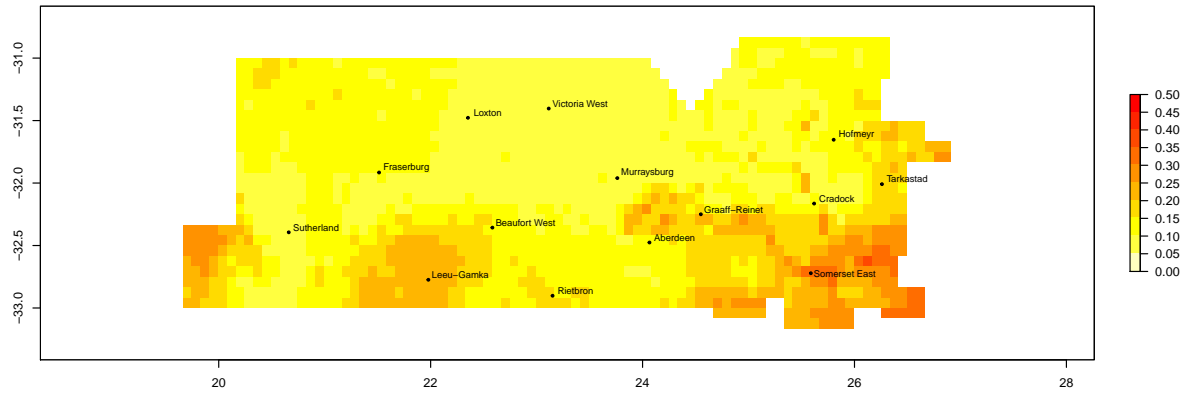
Opisthophthalmus crassimanus



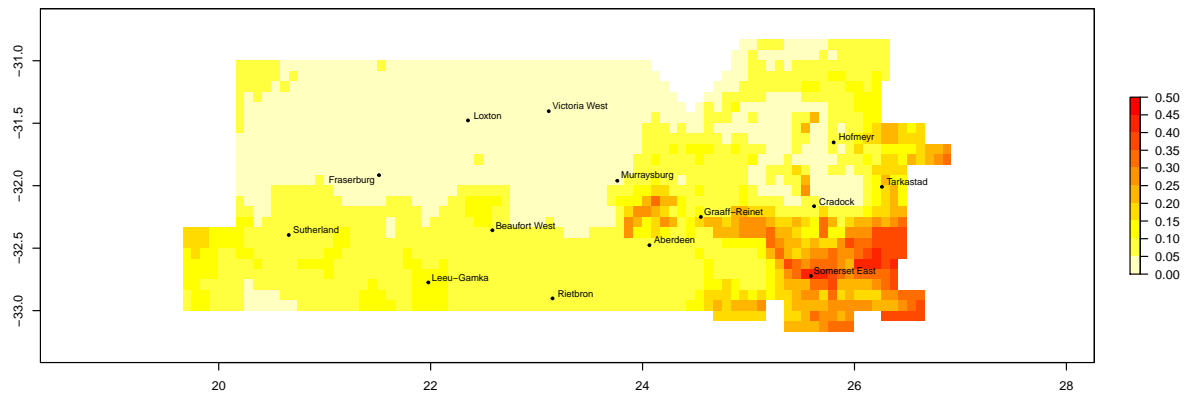
Opisthophthalmus karrooensis



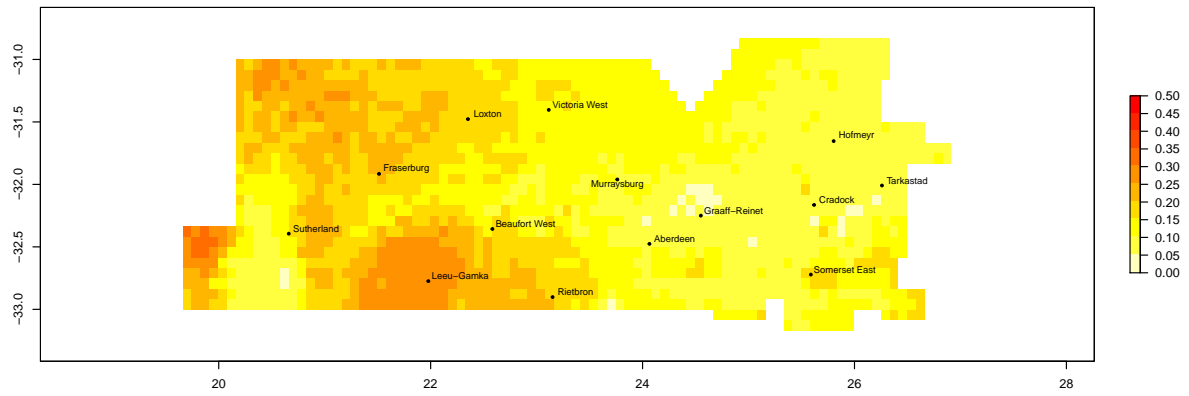
Opisthophthalmus laticauda



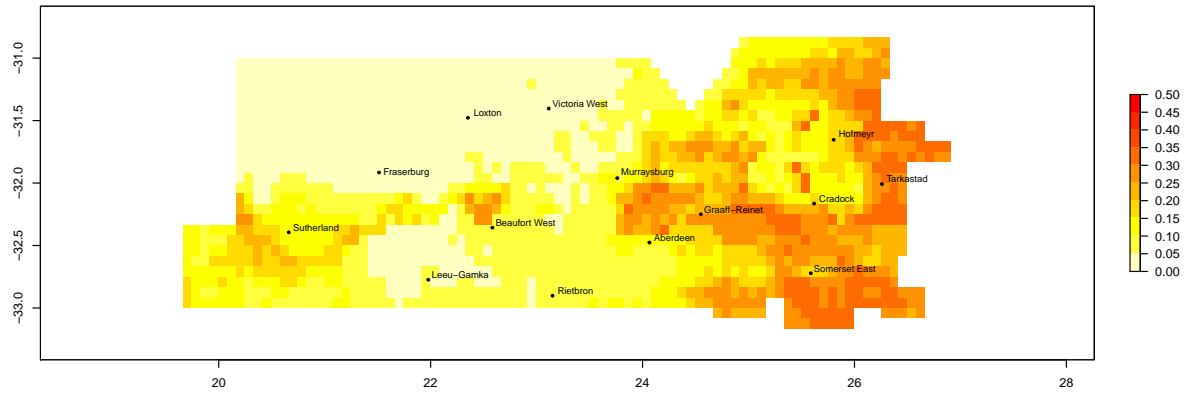
Opisthophthalmus latimanus



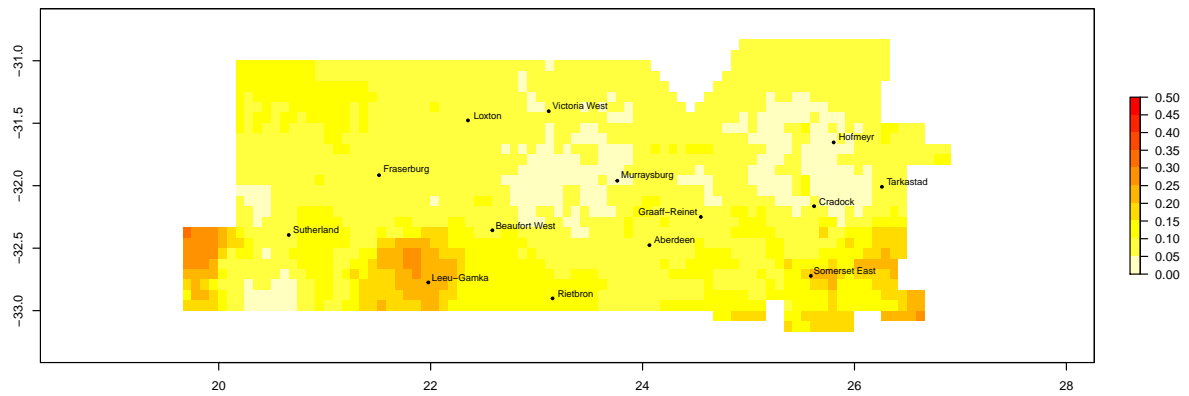
Opisthophthalmus lornae



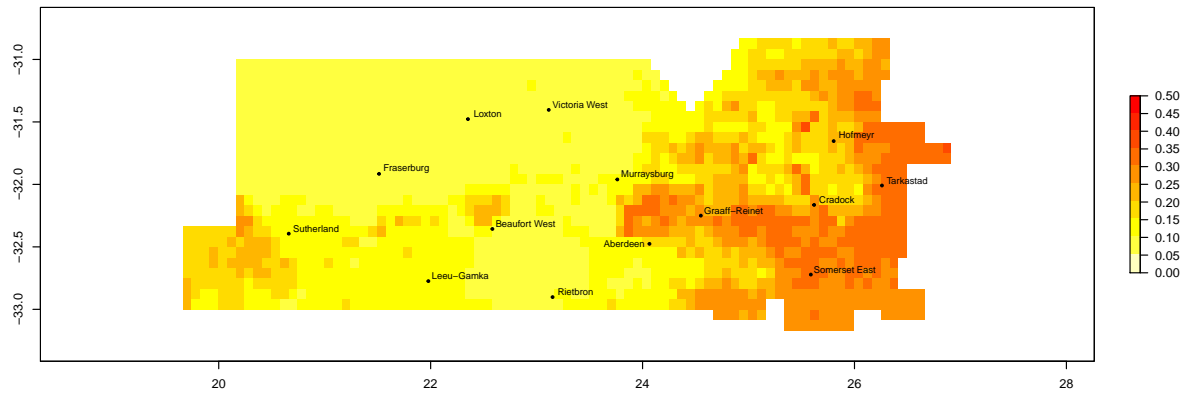
Opisthophthalmus nitidiceps



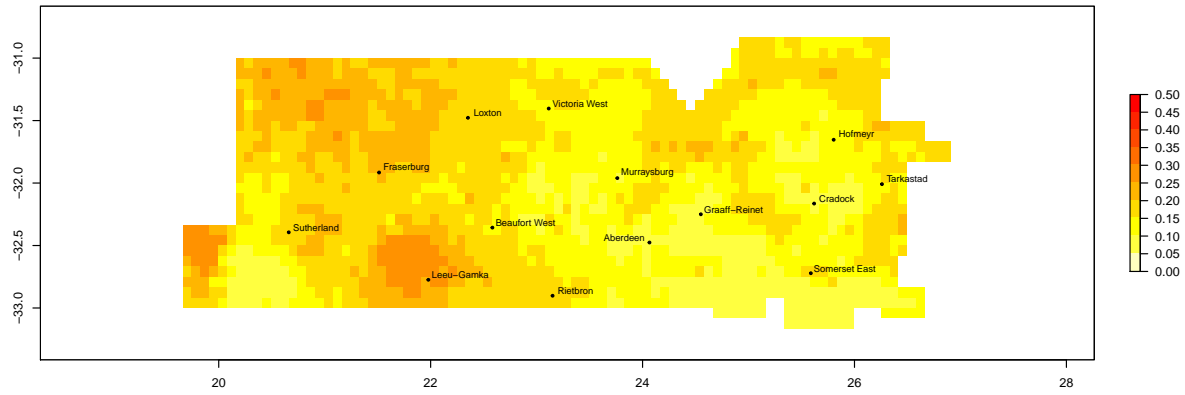
Opisthophthalmus pallipes



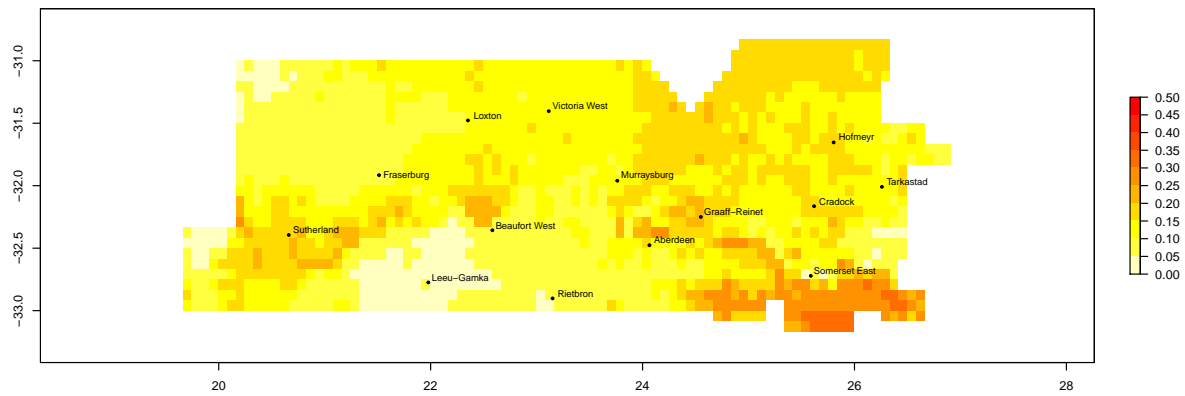
Opisthophthalmus pictus



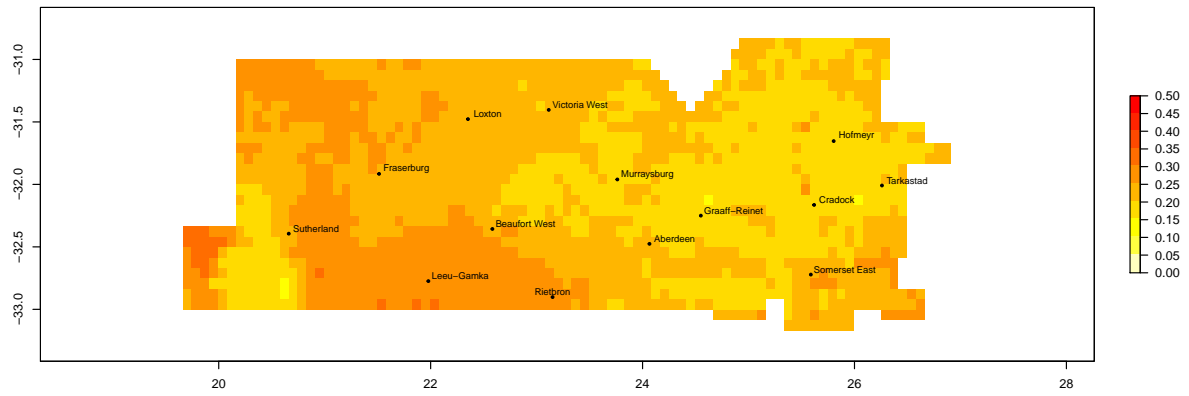
***Opisthophthalmus* sp.**



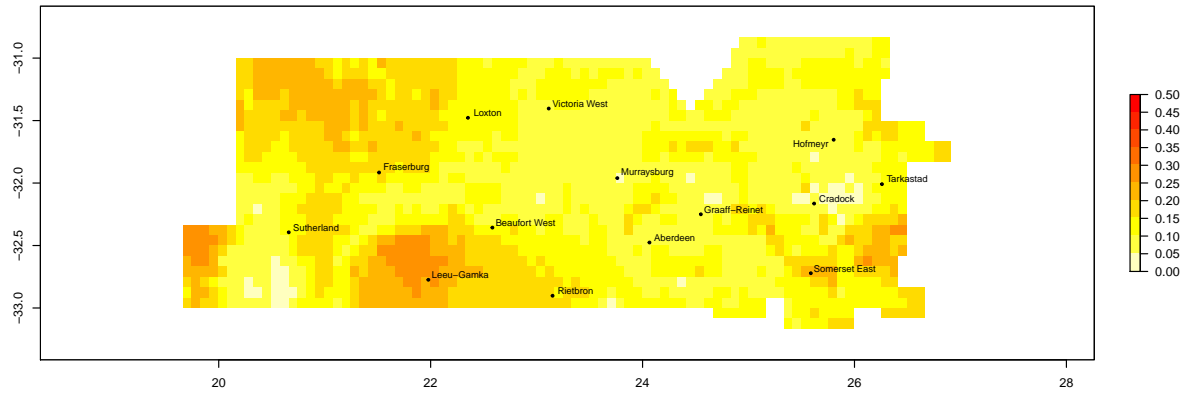
Parabuthus capensis



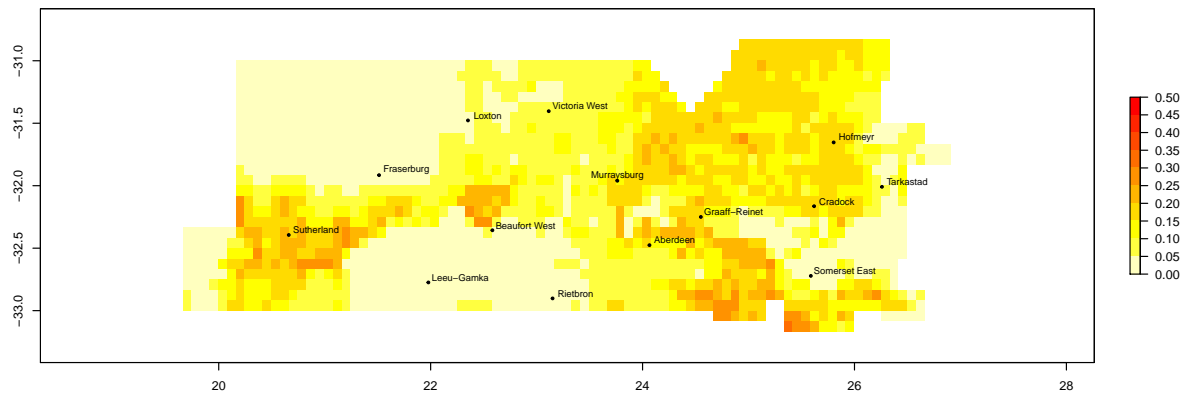
Parabuthus granulatus



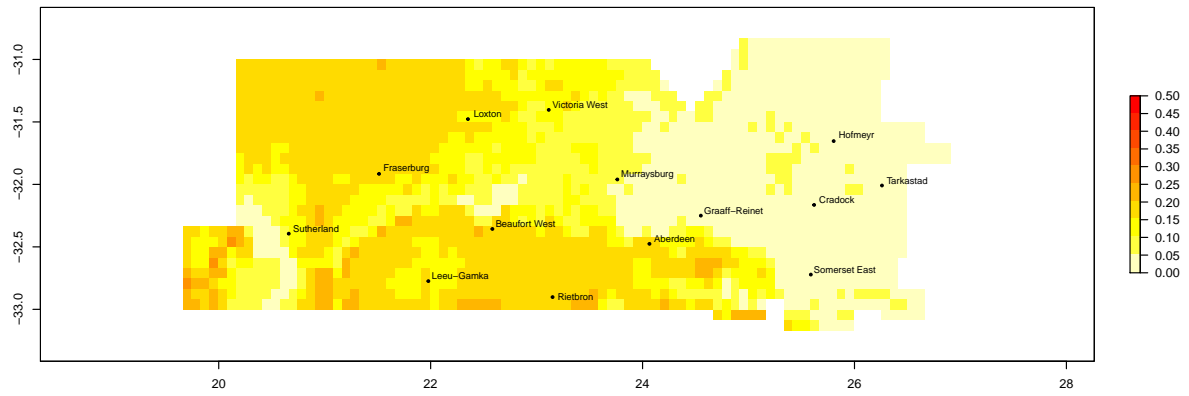
Parabuthus nanus



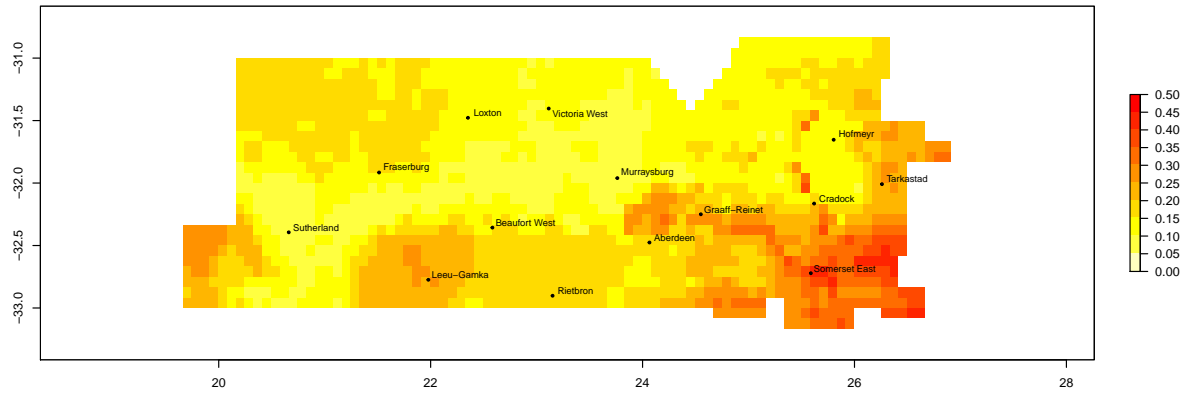
Parabuthus planicauda



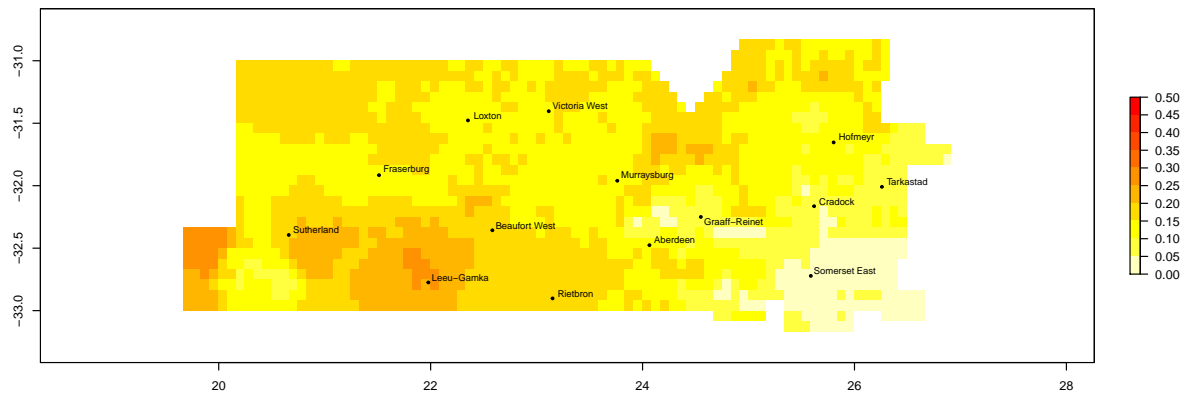
Parabuthus schlechteri



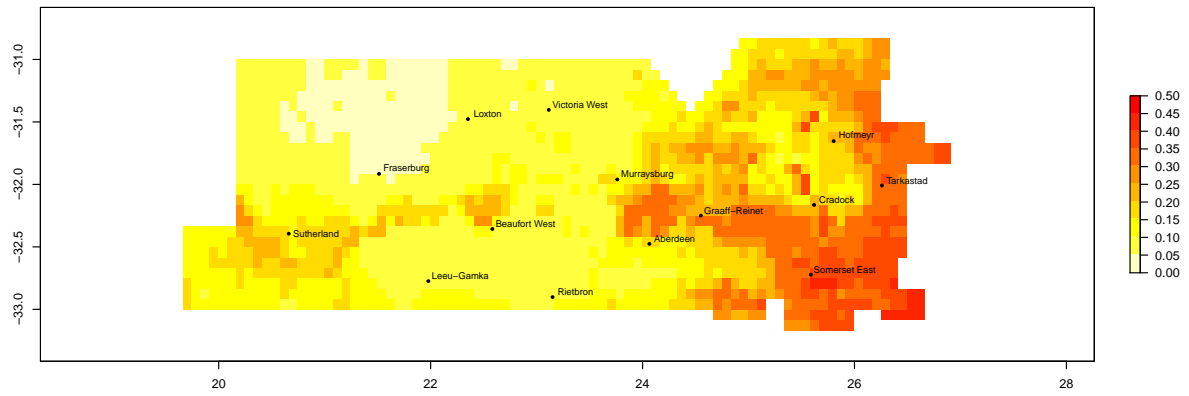
Uroplectes ansiedippenarae



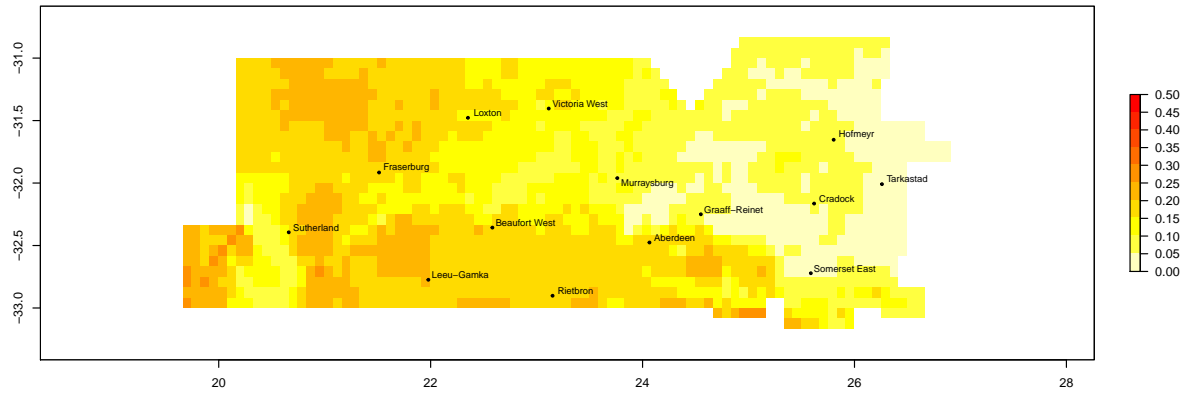
Uroplectes carinatus



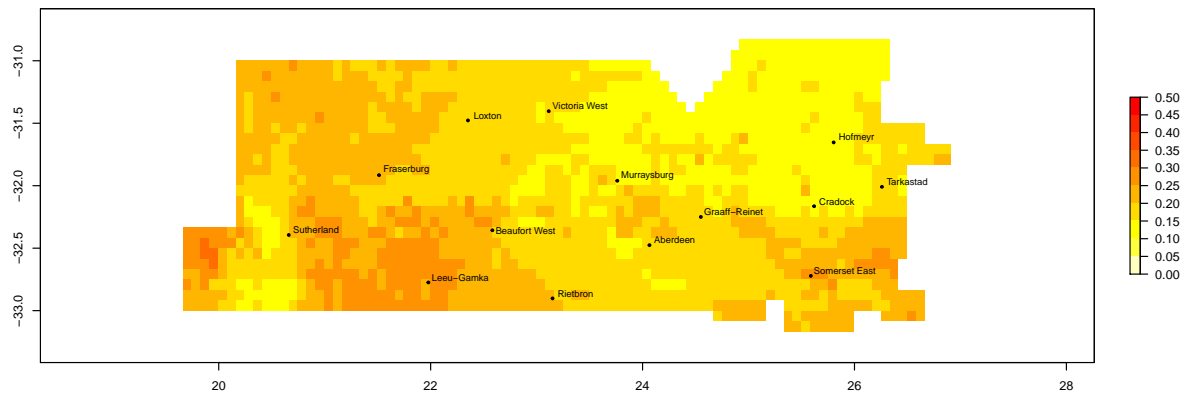
Uroplectes formosus

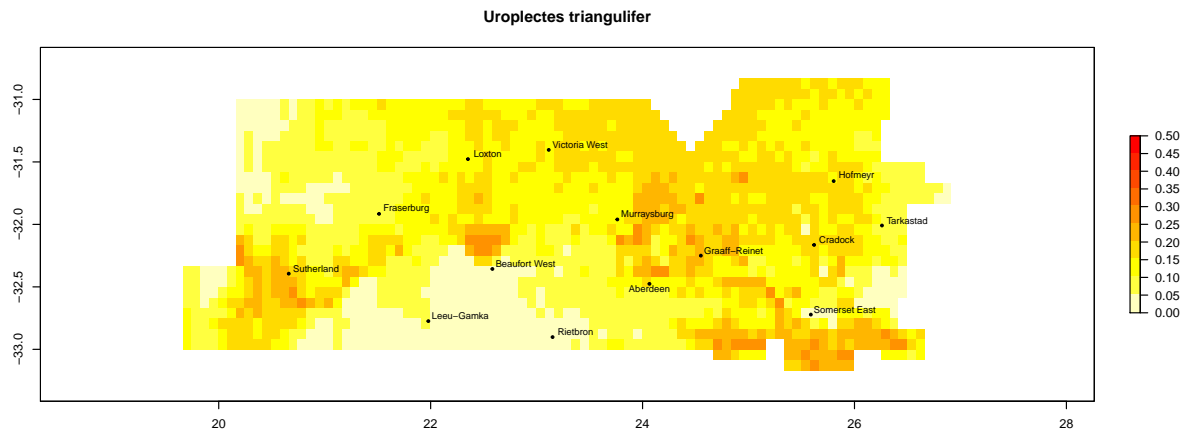


Uroplectes gracilior



Uroplectes schlechteri





6 Appendices

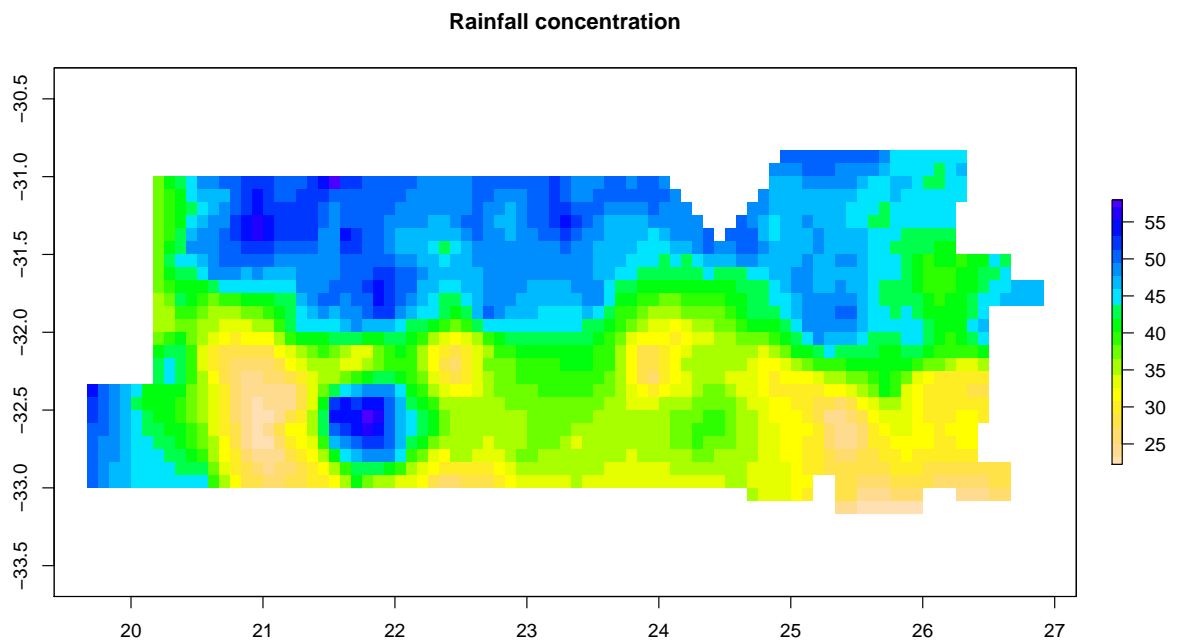
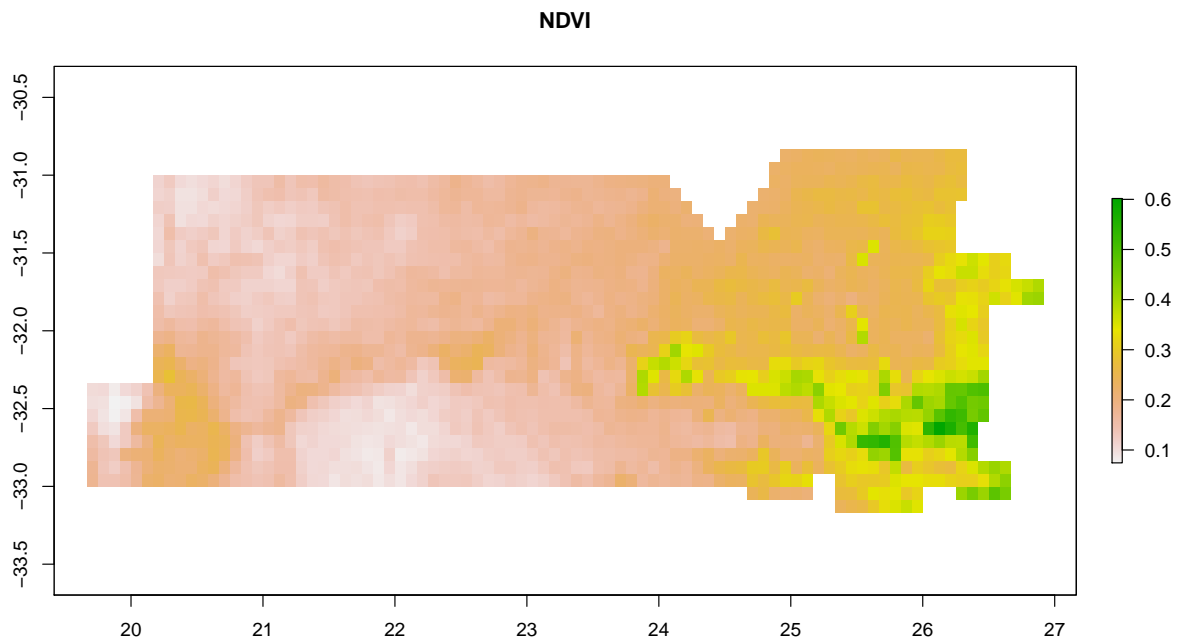
6.1 Appendix A - Species list

List of scorpion species recorded during the fieldwork surveys.

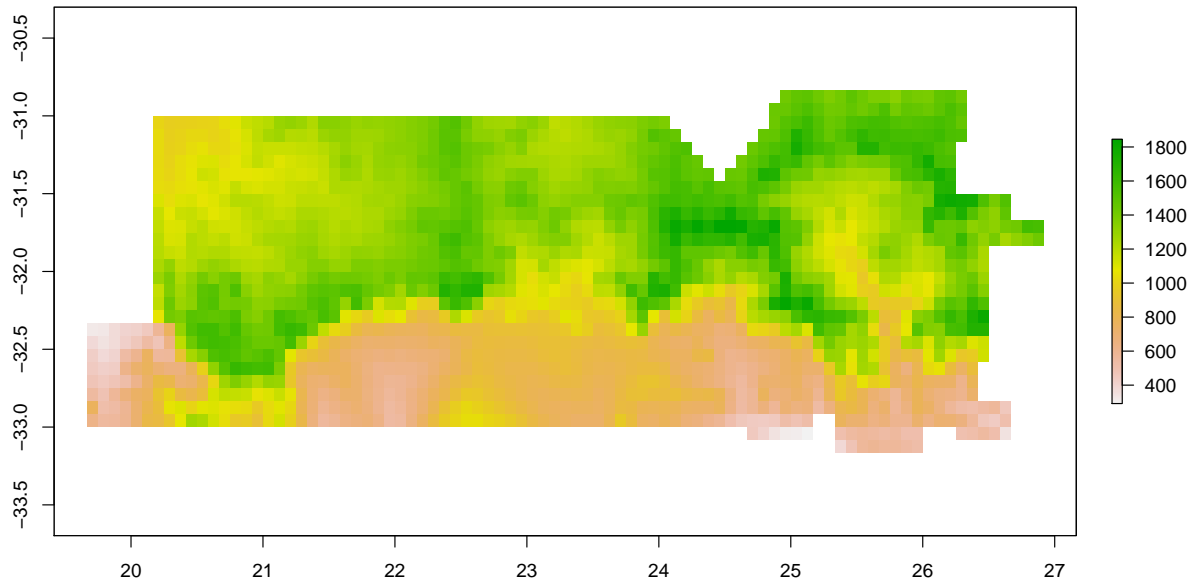
Species
Hadogenes sp.
Hadogenes trichiurus
Opisthacanthus validus
Opisthophthalmus austeroides
Opisthophthalmus austerus
Opisthophthalmus crassimanus
Opisthophthalmus karrooensis
Opisthophthalmus laticauda
Opisthophthalmus latimanus
Opisthophthalmus lornae
Opisthophthalmus nitidiceps
Opisthophthalmus pallipes
Opisthophthalmus pictus
Opisthophthalmus sp.
Parabuthus capensis
Parabuthus granulatus
Parabuthus nanus
Parabuthus planicauda
Parabuthus schlechteri
Uroplectes ansiedippenaarae
Uroplectes carinatus
Uroplectes formosus
Uroplectes gracilior
Uroplectes schlechteri
Uroplectes triangulifer

6.2 Appendix B - Covariate maps

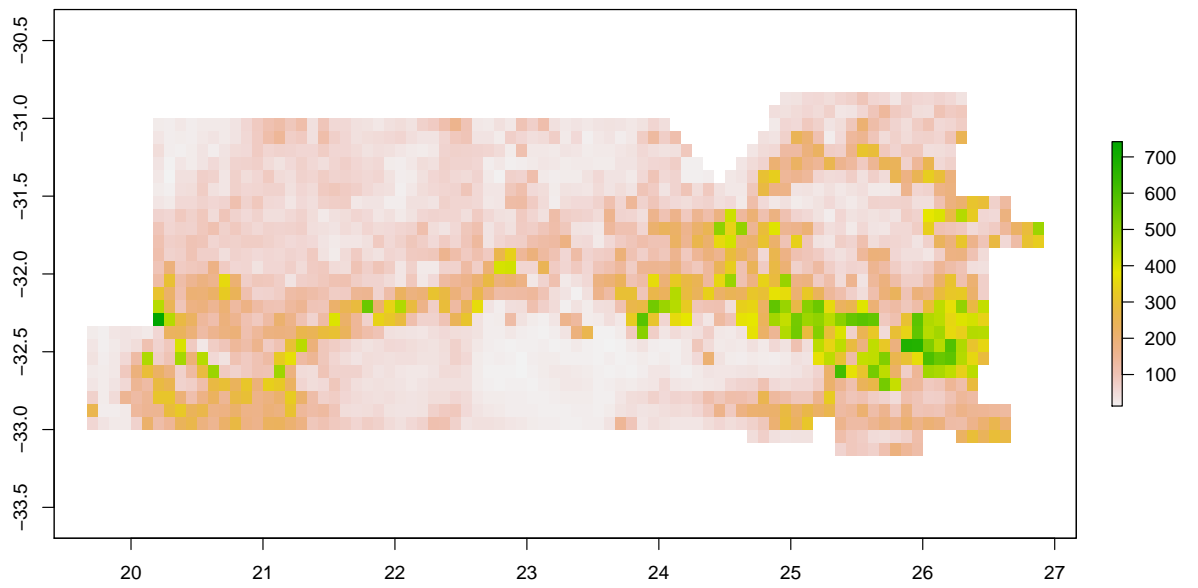
Maps of environmental covariates across the BioGaps study area.



Elevation



TRI



6.3 Appendix C - Model diagnostics

These plots show the posterior distribution of each derived model parameter. Following these are traceplots show R-hat values and diagnostics of parameter convergence. **Add explanation/key about parameter names**

